normal, because we could not recover live offspring in tetraploid complementation experiments, which indicates that mGS cells alone cannot produce a normal whole embryo. The failure is most likely related to the imprint status of mGS cells, since altered imprinted gene methylation causes fetal abnormalities with ES cells (Dean et al., 1998; Surani, 2001). Nevertheless, the imprint status of mGS cells did not influence the germline competence, and normal offspring were obtained from the chimeric animal. This agrees with the previous reports that both ES and EG cells can produce germline chimera (Robertson and Bradley, 1986; Labosky et al., 1994; Stewart et al., 1994), even with androgenetic imprint patterns (Narasimha et al., 1997).

The derivation of multipotent stem cells from the neonatal testis may have practical value for medicine and biotechnology. These cells are different from other reported multipotent cells in terms of morphology, marker expression, and capacity for differentiation (Verfaillie, 2002; Wagers and Weissman, 2004). While it is important to study the biology of individual cell types and assess their potential for clinical application, a major advantage of mGS cells is that techniques currently used to derive specific lineages of cells from ES cells are applicable directly. Clearly, the derivation of mGS cells has fewer ethical concerns than does the derivation of ES cells, because mGS cells can be obtained without sacrificing the conceptus or embryos. Furthermore, the availability of histocompatible, multipotent tissue for autotransplantation would circumvent immunological problems associated with ES cell-based technology. Although we failed to obtain mGS cells from mature wild-type animals, this was likely due to the low success rate of GS cell establishment. The results of the p53 knockout mouse experiment suggest that mGS cells can arise from mature testis. Development of more efficient systems to derive GS cells from mature testis is necessary at this stage of research, and suppression of p53 expression in GS cells, such as by RNA interference, may be useful for enhancing the frequency of derivation. Future studies should also be directed toward examining the effect of imprinting on the range and efficiency of differentiation. Such studies will provide important information for potential clinical applications.

Experimental Procedures

Cell Culture

Testis cells were collected from newborn (0–2 days old) ddY or DBA/2 mice (Japan SLC, Shizuoka, Japan). For some experiments, testis cells were collected from a newborn Green mouse (Kanatsu-Shinohara et al., 2003a) or p53 knockout mouse in ICR background (Tsukada et al., 1993). Testis cell culture was performed according to the previously published protocol (Kanatsu-Shinohara et al., 2003a), with slight modifications. In brief, testis cells were allocated to a gelatin-coated tissue culture plate (2×10^5 cells/3.8 cm^2). The next day, floating cells were recovered and passed to secondary culture plates. After 7 days in culture, the cells were passed to a fresh culture plate at a 1:2 dilution. When the cells were confluent (~7 days after the second passage), they were passed again (1:1 dilution). At the third or fourth passage, the cells were maintained on mitomycin C-inactivated MEF. ES-like cells were cultured in Dulbecco's modified Eagle's medium supplemented with 15% FCS, 5×10^{-5} M 2-mercaptoethanol, and 10^3 units/ml ESGRO (Invitrogen, Carlsbad, CA). To induce EG cells from neonatal testis, the same medium was also supplemented with 20 ng/ml human bFGF (Invitrogen), and cells were cultured on SI⁴-m220 (gift from Dr. T. Nakano, Osaka University).

For adult testis culture, 2×10^7 cells from 3- to 8-week-old wild-type and p53 knockout mice were used to recover spermatogonial stem cells with anti-CD9 antibody as described elsewhere (Kanatsu-Shinohara et al., 2004), and selected cells were plated on gelatin-coated plate (3×10^5 cells/9.5 cm^2). GS cell colonies were picked by micromanipulation and transferred to MEF for expansion.

Standard ES cell medium was used to culture D3 ES cells that ubiquitously express the EGFP gene under the CAG promoter (provided by Dr. M. Okabe, Osaka University; Niwa et al., 1991).

Antibodies and Staining

The following primary antibodies were used: rat anti-EpCAM (G8.8), mouse anti-SSEA-1 (MC-480), mouse anti-sarcomeric protein (MF20; Developmental Studies Hybridoma Bank, University of Iowa), rat anti-mouse Forssman antigen (M1/87), rat anti-human α6-integrin (GoH3), biotinylated hamster anti-rat β1-integrin (Ha2/5), biotinylated rat anti-mouse CD9 (KMC8), allophycocyanin (APC)-conjugated rat anti-mouse c-kit (2B8), rat anti-mouse CD31 (MEC 13.3), phycoerythrin (PE)-conjugated rat anti-mouse Ter119 (TER-119), biotinylated rat anti-mouse Mac1 (M1/70), biotinylated rat anti-mouse Gr1 (RB6-8C5), rat anti-mouse VE-cadherin (11D4.1), APC-conjugated rat anti-mouse CD45 (30-F11; BD Biosciences), rat anti-TDA (EE2; provided by Dr. Y. Nishimune, Osaka University), APC-conjugated rat anti-mouse Flk-1 (Avas 12α1; provided by Dr. S. Nishikawa, RIKEN), goat anti-mouse cardiac troponin-I (cTn-I) (Santa Cruz Biotechnology, Santa Cruz, CA), mouse anti-human myosin light chain 2v (MLC2v) (Alexis Biochemicals Inc, Montreal, Canada), rabbit anti-mouse atrial natriuretic peptide (ANP) (Protos Biotech Corporation, NY), mouse anti-human myelin basic protein (MBP) (Pm43), rabbit anti-glial fibrillary acidic protein (GFAP), rabbit anti-mouse tyrosine hydroxylase (TH), and mouse anti-human β-tubulin III (Tuj) (SDL.3D10) (Sigma, St. Louis, MO). APC-conjugated goat anti-rat-IgG (Cedarlane Laboratories, ON, Canada), APC-conjugated streptavidin (BD Biosciences), Alexa Fluor 488-conjugated goat anti-mouse IgG, Alexa Fluor 647-conjugated goat anti-rat IgM, Alexa Fluor 633-conjugated goat anti-mouse IgM (Molecular Probes, Eugene, OR), Cy3-conjugated donkey anti-mouse IgG, Cy3-conjugated donkey anti-rabbit IgG, ALP or peroxidase-conjugated donkey anti-mouse IgG, ALP-conjugated donkey anti-rabbit IgG (Jackson Immunoresearch, West Grove, PA), ALP-conjugated rabbit anti-goat IgG (Vector Laboratories, Burlingame, CA), or ALP-conjugated goat anti-rat IgG (Chemicon) were used as secondary antibodies. The cell staining and analysis was carried out with a FACSCalibur system (BD Biosciences) (Kanatsu-Shinohara et al., 2003a). ALP or DAB staining was carried out using a VECTOR alkaline phosphatase substrate kit or DAB substrate kit (Vector Laboratories), respectively, according to manufacturer's protocol.

Differentiation into Specific Lineages In Vitro

For differentiation into mesodermal lineages, ES-like cells were cultured on OP9 feeder layers, and cell differentiation was induced as described (Nishikawa et al., 1998; Schroeder et al., 2003, Hirashima et al., 1999). Vascular cells were identified by the uptake of DiI-acetylated low-density lipoprotein (Molecular Probes). Methylcellulose culture was performed as described previously (Nishikawa et al., 1998). All cytokines were provided by Kirin Brewery (Tokyo, Japan). Neural cell differentiation was induced as previously described (Ying et al., 2003).

Analysis of Marker Gene Expression

RT-PCR for Nanog, Rex-1, ERas, Esg-1, Cripto, and ZFP57 were carried out using specific primers, as described (Mitsui et al., 2003; Goolsby et al., 2003; Takahashi et al., 2003; Tanaka et al., 2002; Kimura et al., 2001; Ahn et al., 2004). PCR amplifications for Oct-4, UTF1, and HPRT were carried out by using specific primers (5′-AGCTGCTGAAGCAGAAGAGG-3′ and 5′-GGTTCTCATTGTTGTCG GCT-3′ for Oct-4, 5′-GATGTCCCGGTGACTACGTCT-3′ and 5′-TCG GGGAGGATTCGAAGGTAT-3′ for UTF1, and 5′-GCTGGTGAAAAG GACCTCT -3′ and 5′- CACAGGACTAGAACACCTGC-3′ for HPRT).

Analysis of Imprinted Genes

Bisulfite genomic sequencing of DMRs of imprinted genes was carried out as described (Lee et al., 2002). PCR amplifications of each DMR region from bisulfite-treated genomic DNAs was carried out by using specific primers (5′-GGAATATTTGTGTTTTTGGAGGG-3′ and 5′-AATTTGGGTTGGAGATGAAAATATTG-3′ for *H19*, 5′-GGTTTGGTATATATGGATGTATTGTAATATAGG-3′ and 5′-ATAAAACACCAAATCTATACCAAAATATACC-3′ for *Meg3 IG*, 5′-GTGTAGAATATGGGGTTGTTTTATATTG-3′ and 5′-ATAATACAACAACAACAATAACAATC-3′ for *Rasgrf1*, 5′-TTAGTGGGGTATTTTTATTTGTATGG-3′ and 5′-AAATATCCTAAAAATACAAACTACACAA-3′ for *Igf2r*, 5′-GTAAAGTGATTGGTTTTGTATTTTTAAGTG-3′ and 5′-TTAATTACTCTCCTACAACTTTCCAAATT-3′ for *Peg10*, and 5′- GGTTTTTTAGAG GATGGTTGAGTG-3′ and 5′- TCCAACCCTACTAACCCATCACC-3′ for *Oct-4*). The DNA sequences were determined in both directions. For COBRA, PCR products were digested with restriction enzymes with a recognition sequence containing CpG in the original unconverted DNA (Xiong and Laird, 1997). Intensity of digested DNA bands was quantified with ImageGauge software (Fuji Photo Film, Tokyo, Japan).

Transplantation

For subcutaneous injections, approximately 2×10^6 cells were injected into KSN nude mice (Japan SLC). For microinjections into the seminiferous tubules, approximately 3×10^5 cells were injected into the seminiferous tubules of an immune-suppressed W mouse (Japan SLC) recipient through the efferent duct (Kanatsu-Shinohara et al., 2003b).

Chimera Formation and Microinsemination

Cells were injected into the blastocoel of 3.5 dpc blastocysts of C57BL/6 mice using a Piezo-driven micromanipulator (Kimura and Yanagimachi, 1995). The blastocysts were returned to the oviducts or uteri of 2.5 dpc pseudopregnant ICR foster mothers on the day of microinjection. Tetraploid embryo aggregation chimeras were produced using the method developed by Nagy et al. (1993), except that two-cell blastomeres were electrofused by applying an electric pulse (2500 V/cm, 10 μsec) in 300 mM mannitol solution. Microinsemination was carried out as described using BDF1 oocytes (Kimura and Yanagimachi, 1995). The embryos were transferred on the next day after culture.

Histology

Tissues were fixed in 10% formalin and processed for paraffin sectioning. Chimeric embryos were fixed in 4% paraformaldehyde and frozen in Tissue-Tek OCT compound (Sakura Finetechnical, Tokyo, Japan) for cryosectioning. Slides were analyzed with an Olympus confocal laser scanning microscope.

Acknowledgments

We declare that none of the authors have a financial interest related to this work. We thank Drs. Y. Kaziro and Y. Matsui for discussion and encouragement, and Ms. A. Wada for technical assistance. Financial support for this research was provided by the Inamori Foundation; the Ministry of Health and Welfare; and the Ministry of Education, Culture, Sport, Science, and Technology of Japan.

Received: April 30, 2004
Revised: October 7, 2004
Accepted: November 2, 2004
Published: December 28, 2004

References

Ahn, J.-I., Lee, K.-H., Shin, D.-M., Shim, J.-W., Lee, J.-S., Chang, S.Y., Lee, Y.-S., Brownstein, M.J., Lee, S.-H., and Lee, Y.-S. (2004). Comprehensive transcriptome analysis of differentiation of embryonic stem cells into midbrain and hindbrain neurons. Dev. Biol. *265*, 491–501.

Anderson, R., Schaible, K., Heasman, J., and Wylie, C.C. (1999). Expression of the homophilic adhesion molecule, Ep-CAM, in the mammalian germ line. J. Reprod. Fertil. *116*, 379–384.

Brinster, R.L., and Avarbock, M.R. (1994). Germline transmission of donor haplotype following spermatogonial transplantation. Proc. Natl. Acad. Sci. USA *91*, 11303–11307.

Brinster, R.L., and Zimmermann, J.W. (1994). Spermatogenesis following male germ-cell transplantation. Proc. Natl. Acad. Sci. USA *91*, 11298–11302.

Chambers, I., Colby, D., Robertson, M., Nichols, J., Lee, S., Tweedie, S., and Smith, A. (2003). Functional expression cloning of Nanog, a pluripotency sustaining factor in embryonic stem cells. Cell *113*, 643–655.

Davis, T.L., Trasler, J.M., Moss, S.B., Yang, G.J., and Bartolomei, M.S. (1999). Acquisition of the H19 methylation imprint occurs differentially on the parental alleles during spermatogenesis. Genomics *58*, 18–28.

Davis, T.L., Yang, G.J., McCarrey, J.R., and Bartolomei, M.S. (2000). The H19 methylation imprint is erased and re-established differentially on the parental alleles during male germ cell development. Hum. Mol. Genet. *9*, 2885–2894.

Dean, W., Bowden, L., Aitchison, A., Klose, J., Moore, T., Menesses, J.J., Reik, W., and Feil, R. (1998). Altered imprinted gene methylation and expression in completely ES cell-derived mouse fetuses: association with aberrant phenotypes. Development *125*, 2273–2282.

de Rooij, D.G., and Russell, L.D. (2000). All you wanted to know about spermatogonia but were afraid to ask. J. Androl. *21*, 776–798.

Evans, M.J., and Kaufman, M.H. (1981). Establishment in culture of pluripotential cells from mouse embryos. Nature *292*, 154–156.

Goolsby, J., Marty, M.C., Heletz, D., Chiappelli, J., Tashko, G., Yarnell, D., Fishman, P.S., Dhib-Jalbut, S., Bever, C.T., Jr., and Trister, D. (2003). Hematopoietic progenitors express neural genes. Proc. Natl. Acad. Sci. USA *100*, 14926–14931.

Hattori, N., Nishino, K., Ko, Y.-G., Hattori, N., Ohgane, J., Tanaka, S., and Shiota, K. (2004). Epigenetic control of mouse Oct-4 gene expression in embryonic stem cells and trophoblast stem cells. J. Biol. Chem. *279*, 17063–17069.

Hirashima, M., Kataoka, H., Nishikawa, S., Matsuyoshi, N., and Nishikawa, S.-I. (1999). Maturation of embryonic stem cells into endothelial cells in an in vitro model of vasculogenesis. Blood *93*, 1253–1263.

Humpherys, D., Eggan, K., Akutsu, H., Hochedlinger, K., Rideout, W.M., III, Biniszkiewicz, D., Yanagimachi, R., and Jaenisch, R. (2001). Epigenetic instability in ES cells and cloned mice. Science *293*, 95–97.

Kafri, T., Ariel, M., Brandeis, M., Shemer, R., Urven, L., McCarrey, J.R., Ceder, H., and Razin, A. (1992). Developmental pattern of gene-specific DNA methylation in the mouse embryo and germ line. Genes Dev. *6*, 705–714.

Kanatsu, M., and Nishikawa, S.-I. (1996). In vitro analysis of epiblast tissue potency for hematpoietic cell differentiation. Development *122*, 823–830.

Kanatsu-Shinohara, M., Ogonuki, N., Inoue, K., Miki, H., Ogura, A., Toyokuni, S., and Shinohara, T. (2003a). Long-term proliferation in culture and germline transmission of mouse male germline stem cells. Biol. Reprod. *69*, 612–616.

Kanatsu-Shinohara, M., Ogonuki, N., Inoue, K., Ogura, A., Toyokuni, S., Honjo, T., and Shinohara, T. (2003b). Allogeneic offspring produced by male germ line stem cell transplantation into infertile mouse testis. Biol. Reprod. *68*, 167–173.

Kanatsu-Shinohara, M., Toyokuni, S., and Shinohara, T. (2004). CD9 is a surface marker on mouse and rat male germline stem cells. Biol. Reprod. *70*, 70–75.

Kimura, Y., and Yanagimachi, R. (1995). Mouse oocytes injected with testicular spermatozoa or round spermatids can develop into normal offspring. Development *121*, 2397–2405.

Kimura, C., Shen, M.M., Takeda, N., Aizawa, S., and Matsuo, I. (2001). Complementary functions of Otx2 and Cripto in initial patterning of mouse epiblast. Dev. Biol. *235*, 12–32.

Koshimizu, U., Nishioka, H., Watanabe, D., Dohmae, K., and Nishimune, Y. (1995). Characterization of a novel spermatogenic cell antigen specific for early stages of germ cells in mouse testis. Mol. Reprod. Dev. *40*, 221–227.

Labosky, P.A., Barlow, D.P., and Hogan, B.L.M. (1994). Mouse embryonic germ (EG) cell lines: transmission through the germline and differences in the methylation imprint of insulin-like growth factor 2 receptor (Igf2r) gene compared with embryonic stem (ES) cell lines. Development *120*, 3197–3204.

Lam, M.-Y.J., and Nadeau, J.H. (2003). Genetic control of susceptibility to spontaneous testicular germ cell tumors in mice. APMIS *111*, 184–191.

Lee, J., Inoue, K., Ono, R., Ogonuki, N., Kohda, T., Kaneko-Ishino, T., Ogura, A., and Ishino, F. (2002). Erasing genomic imprinting memory in mouse clone embryos produced from day 11.5 primordial germ cells. Development *129*, 1807–1817.

Liu, X., Wu, H., Loring, J., Hormuzdi, S., Disteche, C.M., Bornstein, P., and Jaenisch, R. (1997). Trisomy eight in ES cells is a common potential problem in gene targeting and interferes with germ line transmission. Dev. Dyn. *209*, 85–91.

Longo, L., Bygrave, A., Grosveld, F.G., and Pandolfi, P.P. (1997). The chromosome make-up of mouse embryonic stem cells is predictive of somatic and germ cell chimaerism. Transgenic Res. *6*, 321–328.

Martin, G.R. (1981). Isolation of a pluripotent cell line from early mouse embryos cultured in medium conditioned by teratocarcinoma stem cells. Proc. Natl. Acad. Sci. USA *78*, 7634–7638.

Matsui, Y., Zsebo, K., and Hogan, B.L.M. (1992). Derivation of pluripotential embryonic stem cells from murine primordial germ cells in culture. Cell *70*, 841–847.

Meistrich, M.L., and van Beek, M.E.A.B. (1993). Spermatogonial stem cells. In Cell and Molecular Biololgy of the Testis, C. Desjardins, and L.L. Ewing, eds. (New York: Oxford University Press), pp. 266–295.

Meng, X., Lindahl, M., Hyvönen, M.E., Parvinen, M., de Rooij, D.G., Hess, M.W., Raatikainen-Ahokas, A., Sainio, K., Rauvala, H., Lakso, M., et al. (2000). Regulation of cell fate decision of undifferentiated spermatogonia by GDNF. Science *287*, 1489–1493.

Mitsui, K., Tokuzawa, Y., Itoh, H., Segawa, K., Murakami, M., Takahashi, K., Maruyama, M., Maeda, M., and Yamanaka, S. (2003). The homeoprotein Nanog is required for maintenance of pluripotency in mouse epiblast and ES cells. Cell *113*, 631–642.

Nagy, A., Rossant, J., Nagy, R., Abramow-Newerly, A., and Roder, J.C. (1993). Derivation of completely cell culture-derived mice from early-passage embryonic stem cells. Proc. Natl. Acad. Sci. USA *90*, 8424–8428.

Nakano, T., Kodama, H., and Honjo, T. (1994). Generation of lymphohematopoietic cells from embryonic stem cells in culture. Science *265*, 1098–1101.

Narasimha, M., Barton, S.C., and Surani, M.A. (1997). The role of the paternal genome in the development of the mouse germ line. Curr. Biol. *7*, 881–884.

Nishikawa, S.-I., Nishikawa, S., Hirashima, M., Matsuyoshi, N., and Kodama, H. (1998). Progressive lineage analysis by cell sorting and culture identifies FLK1$^+$VE-cadherin$^+$ cells at a diverging point of endothelial and hemopoietic lineages. Development *125*, 1747–1757.

Niwa, H., Yamamura, K., and Miyazaki, J. (1991). Efficient selection for high-expression transfectants with a novel eukaryotic vector. Gene *108*, 193–200.

Okuda, A., Fukushima, A., Nishimoto, M., Orimo, A., Yamagishi, T., Nabeshima, Y., Kuro-o, M., Nabeshima, Y., Boon, K., Keaveney, M., et al. (1998). UTF1, a novel transcriptional coactivator expressed in pluripotent embryonic stem cells and extra-embryonic cells. EMBO J. *17*, 2019–2032.

Pesce, M., and Schöler, H.R. (2001). Oct-4: gatekeeper in the beginning of mammalian development. Stem Cells *19*, 271–278.

Resnick, J.L., Bixler, L.S., Cheng, L., and Donovan, P.J. (1992). Long-term proliferation of mouse primordial germ cells in culture. Nature *359*, 550–551.

Robertson, E.J., and Bradley, A. (1986). Production of permanent cell lines from early embryos and their use in studying developmental problems. In Experimental Approaches to Mammalian Embryonic Development, J. Rossant, and R.A. Pedersen, eds. (Cambridge: Cambridge University Press), pp. 475–508.

Schrans-Stassen, B.H.G.J., van de Kant, H.J.G., de Rooij, D.G., and van Pelt, A.M.H. (1999). Differential expression of c-kit in mouse undifferentiated and differentiating type A spermatogonia. Endocrinology *140*, 5894–5900.

Schroeder, T., Fraser, S.T., Ogawa, M., Nishikawa, S., Oka, C., Bornkamm, G.W., Nishikawa, S.-I., Honjo, T., and Just, U. (2003). Recombination signal sequence-binding protein Jκ alters mesodermal cell fate decisions by suppressing cardiomyogenesis. Proc. Natl. Acad. Sci. USA *100*, 4018–4023.

Smith, A.G. (2001). Embryo-derived stem cells: of mice and men. Annu. Rev. Cell Dev. Biol. *17*, 435–462.

Solter, D., and Knowles, B.B. (1978). Monoclonal antibody defining a stage-specific mouse embryonic antigen (SSEA-1). Proc. Natl. Acad. Sci. USA *75*, 5565–5569.

Stevens, L.C. (1984). Spontaneous and experimentally induced testicular teratomas in mice. Cell Differ. *15*, 69–74.

Stevens, L.C., and Mackensen, J.A. (1961). Genetic and environmental influences on teratocarcinoma in mice. J. Natl. Cancer Inst. *27*, 443–453.

Stewart, C.L., Gadi, I., and Bhatt, H. (1994). Stem cells from primordial germ cells can reenter the germline. Dev. Biol. *161*, 626–628.

Surani, M.A. (2001). Reprogramming of genome function through epigenetic inheritance. Nature *414*, 122–128.

Takahashi, K., Mitsui, K., and Yamanaka, S. (2003). Role of ERas in promoting tumor-like properties in mouse embryonic stem cells. Nature *423*, 541–545.

Tanaka, T.S., Kunath, T., Kimber, W.L., Jaradat, S.A., Stagg, C.A., Usuda, M., Yokota, T., Niwa, H., Rossant, J., and Ko, M.S.H. (2002). Gene expression profiling of embryo-derived stem cells reveals candidate genes associated with pluripotency and lineage specificity. Genome Res. *12*, 1921–1928.

Tsukada, T., Tomooka, Y., Takai, S., Ueda, Y., Nishikawa, S.-I., Yagi, T., Tokunaga, T., Takeda, N., Suda, Y., Abe, S., et al. (1993). Enhanced proliferative potential in culture of cells from p53-deficient mice. Oncogene *8*, 3313–3322.

Verfaillie, C.M. (2002). Adult stem cells: assessing the case for pluripotency. Trends Cell Biol. *12*, 502–508.

Wagers, A.J., and Weissman, I.L. (2004). Plasticity of adult stem cells. Cell *116*, 639–648.

Xiong, Z., and Laird, P.W. (1997). COBRA: a sensitive and quantitative DNA methylation assay. Nucleic Acids Res. *25*, 2532–2534.

Ying, Q.L., Stavridis, M., Griffiths, D., Li, M., and Smith, A. (2003). Conversion of embryonic stem cells into neuroectodermal precursors in adherent monoculture. Nat. Biotechol. *21*, 183–186.

Reproductive Medicine and Biology 2004; 3: 245–251

Original Article

Fertilization and preimplantation development of mouse oocytes after prolonged incubation with caffeine

PERIYASAMY MANONMANI,[1] HIRONORI OKADA,[1] NARUMI OGONUKI,[2] AKIHIKO UDA,[1] ATSUO OGURA,[2] TAKASHI YOSHIDA[1] and TADASHI SANKAI[1]*

[1]*Tsukuba Primate Center for Medical Science, National Institute of Infectious Diseases, Ibaraki, and* [2]*Bioresource Engineering Division, Bioresource Center, RIKEN Tsukuba Institute, Ibaraki, Japan*

Background and Aims: Previous studies have shown that caffeine might cause artificial dephosphorylation at threonine-14 and tyrosine-15 of the p34cdc2 catalytic subunit of maturation-promoting factor (MPF), elevate MPF activity in metaphase II oocytes cultured for a prolonged period, and that caffeine decreases fragmentation in oocytes cultured for up to 96 h.

Methods: Studies were carried out on: (i) the effect of caffeine on the morphological status of oocytes cultured for 96 h; (ii) the parthenogenetic activation and the fertilization of oocytes incubated in a medium that contained caffeine, and (iii) the fertilization and preimplantation development ability of zona-intact and zona-free oocytes by *in vitro* fertilization (IVF) and by intracytoplasmic sperm injection.

Results: In parthenogenetic activation, the incidence of diploid parthenotes in 24-h caffeine-treated oocytes was significantly higher than 24-h non-treated oocytes. For fertilizability of these oocytes, a significant increase in the fertilization rate resulted from IVF after 12-h caffeine incubation. Although no fertilized eggs were observed after intracytoplasmic sperm injection in 24-h non-treated oocytes, fertilized eggs were observed in caffeine-treated oocytes. MPF activation occurs in relation to nuclear/spindle position, and mitotic spindles and actin filaments determine the site of cleavage during cytokinesis. Spindle disruption does not cause cytofragmentation, but does induce cell cycle arrest.

Conclusion: Based on our results, although caffeine might increase MPF activity, prolonged time in any incubation causes some disruption of cytoskeletal filaments, which might be responsible for the poor development of caffeine-treated oocytes. (Reprod Med Biol 2004; 3: 245–251)

Key words: caffeine, *in vitro* fertilization, intracytoplasmic sperm injections, maturation promoting factor, parthenogenesis.

INTRODUCTION

OOCYTES OF MOST mammals are ovulated at metaphase II, and remain at this stage until activation by penetration of spermatozoon or by artificial means such as parthenogenetic activation.[1,2] Investigations using amphibian oocytes and cytoplasmic transfer revealed that mature oocytes contain a large amount of maturation-promoting factor (MPF) in their cytoplasm that maintains the meiotic arrest of these oocytes.[3–5] MPF is a serine/threonine protein kinase composed of a catalytic subunit, p34cdc2, and a regulatory subunit, cyclin B,[6–8] and is a universal cell cycle regulator of both mitosis and meiosis.

*Correspondence: Dr Tadashi Sankai, Tsukuba Primate Center for Medical Science, National Institute of Infectious Diseases, Hachimandai-1, Tsukuba, Ibaraki 305-0843, Japan.
Email: sankai@nih.go.jp
Received 14 June 2004; accepted 24 August 2004.

Cytoplasmic changes affecting the quality of the oocyte, such as decreased ability for normal fertilization and embryonic development, occur when the arrest period is prolonged.[9,10] Spontaneous oocyte activation[11,12] and subsequent fragmentation, and abnormal cleavage after activation characterized by unequal blastomeres,[10,12] have been observed in oocytes cultured for a prolonged period. Low MPF activity might be one cause of these changes. In general, p34cdc2 is phosphorylated at threonine-14 (T14) and tyrosine-15 (Y15) by the Myt1 and Wee1 kinases after association with cyclin B, and this inactive form, called pre-MPF, accumulates during G_2 phase. Therefore, activation of MPF at the G_2 to M transition depends on dephosphorylation at T14 and Y15 by Cdc25 phosphatase.[13] Kikuchi *et al.*[14] suggested that, in addition to the gradual decrease in cyclin B, this phosphorylation contributes to the decrease in MPF activities, and that artificial dephosphorylation of pre-MPF might increase MPF activity.

Control of oocyte aging could have many advantages for *in vitro* fertilization (IVF), sperm injection and cloning by nuclear transfer. Kikuchi *et al.*[14] found a significant elevation of MPF activity in aged oocytes after artificial dephosphorylation at T14 and Y15 of p34cdc2 as a result of caffeine treatment. Caffeine reportedly induces the T14 and Y15 dephosphorylated form of p34cdc2, resulting in elevation of MPF activity in mammalian cultured cells[15,16] and *Xenopus* oocytes.[17]

We examined the effect of caffeine on the morphological status of oocytes cultured for a prolonged period. Then, we studied the fertilization of oocytes incubated in medium that contained caffeine. Because age-dependent alterations in zonae pellucidae might reduce the fertilizability of an oocyte[18] and because no studies on the effect of caffeine on zonae pellucidae have been reported, we examined the fertilization and preimplantation development abilities of zona-intact and zona-free oocytes by IVF and by intracytoplasmic sperm injection (ICSI).

MATERIALS AND METHODS

Collection of metaphase II-arrested oocytes and treatment with caffeine

FEMALE BDF1 MICE, 2–3 months old, were maintained on a 10-h light cycle at the Tsukuba Primate Center for Medical Science, National Institute of Infectious Diseases, Ibaraki, Japan. Females were induced to superovulate by intraperitoneal injections of 7.5 IU of equine chorionic gonadotropin followed 48 h later by 7.5 IU of human chorionic gonadotropin (hCG). Ovulated oocytes were collected from oviducts 14–16 h after the hCG injection. Oocytes were treated with hyaluronidase (1500 U/mL; Sigma, St. Louis, MO, USA) in TYH medium[19] for a few minutes to completely disperse cumulus cells. After being rinsed in TYH medium, oocytes were incubated at 37°C under 5% CO_2 for 0–96 h in 50 μL of TYH medium with and without 5 mM caffeine under mineral oil.

Observation of morphological changes in oocytes

At 0, 6, 12, 24, 48, 72 and 96 h incubation in the medium with caffeine (hereafter called 0, 6, 12, 24, 48, 72 and 96 h-caffeine group, respectively), the morphological status of metaphase II-arrested oocytes was observed and compared with that of oocytes incubated in the medium without caffeine at the same times (hereafter called 0, 6, 12, 24, 48, 72, and 96 h-no-caffeine group, respectively).

Parthenogenetic activation of oocytes

Oocytes were collected from BDF1 mice and incubated in TYH medium with 5 mM caffeine for 24 h or in TYH medium without caffeine for 0 or 24 h. Oocytes were activated by culturing for 6 h in Ca^{2+}-free TYH medium with 10 mM strontium (Sr^{2+}) and 6.6 μg/mL cytochalasin B (Sigma, St. Louis, MO, USA). Parthenotes with two pronuclei were washed with Whitten's medium[20] and then cultured for 96 h in 50-μL drops of Whitten's medium, covered with mineral oil, at 37°C under 5% CO_2 in air. The parthenotes were observed every 24 h after parthenogenetic stimulus.

In vitro fertilization and development

In vitro fertilization of zona-intact and zona-free oocytes was accomplished as follows. Zona-free oocytes were obtained by treating oocytes in acidic Ringer's solution (137 mM NaCl, 26.8 mM KCl, 1.6 mM $CaCl_2$, 0.49 mM $MgSO_4$, 5.55 mM glucose, 4 mg/mL 40-kDa polyvinylpyrrolidone [PVP], pH 2.5) for a few seconds to dissolve the zona pellucida.[21] Zona-intact and zona-free oocytes were incubated for 0, 6, 12 or 24 h in 50 μL of TYH medium (covered with mineral oil) with and without 5 mM caffeine. Before insemination, all oocytes were placed in TYH medium for 15–30 min.

The spermatozoa used for insemination were collected from the cauda epididymis of mature BDF1 male mice and placed in TYH medium. After 2 h incubation at 37°C under 5% CO_2 in air, the sperm suspension was introduced into 50-μL drops of TYH medium containing 10–20 oocytes each. The final sperm concentration was 600 cells/μL for the zona-intact oocytes and 5 cells/μL for the zona-free oocytes. After 6 h insemination, eggs were washed in Whitten's medium. A Terasaki plate (SUMITOMO BAKELITE Co. Ltd, Tokyo, Japan) was used to culture the individual eggs. The eggs were then transferred individually into 10 μL of Whitten's medium at 37 C under 5% CO_2 in air, and then observed for formation of pronuclei. The embryonic development was observed at 24-h intervals up to 96 h after insemination.

Intracytoplasmic sperm injection and development

Oocytes cultured for 24 h in TYH medium, with and without 5 mM caffeine, were fertilized by ICSI. Microinjection was carried out using a micromanipulation system equipped with a piezo micropipette-drive unit (Prime

Tech, Ibaraki, Japan). The cover of a plastic dish (Falcon no. 1006; Becton Dickinson, Franklin Lakes, NJ, USA) was used as a microinjection chamber. Several small drops, each containing either HEPES-CZB medium for oocytes or 12% PVP for spermatozoa, were placed on the bottom of the dish and covered with mineral oil. A tail of spermatozoon showing apparently normal morphology was inserted tail first into an injection pipette. After the sperm head was separated from the tail by applying a few piezo pulses, it was injected into an oocyte.[22] After 6 h incubation at 37°C under 5% CO_2 in air, oocytes were washed in Whitten's medium and then cultured in Whitten's medium at 37°C under 5% CO_2 in air. The embryonic development was observed at 24-h intervals up to 96 h after sperm injection.

Statistical analysis

A χ^2-test was used for statistical evaluation of the results, as required. Differences giving a probability of $P < 0.05$ were considered to be significant.

RESULTS

TABLE 1 SHOWS the morphological status of metaphase II-arrested oocytes incubated for 0, 6, 12, 24, 48, 72 or 96 h in TYH medium, with and without caffeine. Up to 12 h, all oocytes showed normal morphology. At 24 h, although the rate of morphologically normal oocytes in the caffeine-treated group (100%) was higher than that in the non-treated group (89%), the difference was not statistically significant. At 48 and 72 h, the number of morphologically normal oocytes was significantly higher in the caffeine-treated group. At 96 h, neither group showed any morphologically normal oocytes.

Table 2 shows the observed parthenogenetic activation of non-kept (0 h) oocytes and oocytes incubated for 24 h in TYH medium with and without caffeine. In the 0 h-group, all oocytes showed two pronuclei, and 71% of these oocytes developed to blastocysts. The percentage of diploid parthenotes after 24 h in the caffeine-treated group was significantly higher than that in the non-treated group. In the caffeine-treated group, only 22% of the parthenotes developed to the two-cell stage, and no further development occurred. The diploid parthenotes in the non-treated group, however, did not develop even to the two-cell stage.

Table 3 shows the results of IVF and the pre-implantation development of cumulus-free or zona-free oocytes kept for 6, 12, or 24 h in TYH medium with or without caffeine. In the case of 0 h-groups involving cumulus-free and zona-intact oocytes and involving cumulus- and zona-free oocytes, fertilization rate was 35% and 82%, respectively. No significant difference in either the fertilization rate or development rate was evident between the

Table 1 Morphological status of metaphase II-arrested oocytes incubated in medium with and without caffeine

Medium with (+) or without (−) caffeine	Number of oocytes examined	Number of morphologically normal oocytes at different incubation times (%)						
		0 h	6 h	12 h	24 h	48 h	72 h	96 h
−	47	47 (100)	47 (100)	47 (100)	42 (89.4)	14 (29.8)†	2 (4.2)§	0 (0)
+	52	52 (100)	52 (100)	52 (100)	52 (100)	50 (96.2)‡	25 (48.1)¶	0 (0)

†, ‡, §, ¶Percentage of oocytes significantly differed between † and ‡($P < 0.05$) and between § and ¶($P < 0.01$).

Table 2 Parthenogenetic activation of oocytes incubated in medium with and without caffeine

Medium with (+) or without (−) caffeine	Incubation time (h)	Number of oocytes examined	Number of eggs (%)		Number of parthenotes developed to different stages (%)		
			With 2PN†	Without PN or fragmentation	2-cell	Morula	Blastocyst
−	0	34	34 (100)	0 (0)	34 (100)	33 (97.1)	24 (70.6)
	24	22	11 (50.0)‡	9 (40.9)	0 (0)	0 (0)	0 (0)
+	24	23	19 (82.6)§	4 (17.4)	5 (21.7)	0 (0)	0 (0)

†PN, pronucleus observed; 2PN, two pronuclei observed. ‡, §Percentage of diploid parthenotes significantly differed between ‡ and §($P < 0.05$).

Table 3 *In vitro* fertilization and embryonic development of oocytes incubated in medium with and without caffeine

Medium with (+) or without (–) caffeine	Oocytes	Incubation time (h)	Number of oocytes inseminated	Number of eggs with (%)				Number of embryos developed to different stages (%)		
				Pb2 + 1 or 2PN†	Pb2 + 0 PN	0Pb2 + 1 or 2PN	Total	2-Cell	Morula	Blastocyst
–	Cumulus-free, zona-intact	0	263	53 (20.2)	39 (14.8)	0 (0)	92 (35.0)	51 (19.4)	29 (11.0)	18 (6.8)
		6	46	4 (8.7)	2 (4.3)	0 (0)	6 (13.0)	3 (6.5)	2 (4.3)	0 (0)
		12	29	0 (0)	1 (3.4)	0 (0)	1 (3.4)	0 (0)	0 (0)	0 (0)
		24	135	2 (0.7)	8 (5.9)	2 (1.5)	12 (8.9)	1 (0.7)	0 (0)	0 (0)
	Zona-free	0	266	213 (80.1)	6 (2.3)	0 (0)	219 (82.3)	208 (78.2)	193 (72.6)	165 (62.3)
		6	50	36 (72.0)	2 (4.0)	0 (0)	38 (76.0)	35 (70.0)	25 (50.0)	13 (26.0)
		12	28	8 (28.6)	0 (0)	0 (0)	8 (28.6)‡	1 (3.6)¶	0 (0)	0 (0)
		24	117	1 (0.9)	4 (3.4)	2 (1.7)	7 (6.0)	1 (0.9)	0 (0)	0 (0)
+	Cumulus-free, zona-intact	6	56	4 (7.1)	3 (5.4)	0 (0)	7 (12.5)	2 (3.6)	2 (3.6)	1 (1.8)
		12	39	3 (7.7)	4 (10.3)	0 (0)	7 (17.9)	3 (7.7)	1 (2.6)	0 (0)
		24	136	2 (1.5)	10 (8.1)	3 (2.2)	15 (11.0)	2 (1.5)	0 (0)	0 (0)
	Zona-free	6	50	35 (70.0)	1 (2.0)	0 (0)	36 (72.0)	33 (66.0)	23 (46.0)	16 (32.0)
		12	40	16 (40.0)	0 (0)	0 (0)	16 (40.0)§	13 (32.5)††	2 (5.0)	0 (0)
		24	122	2 (1.6)	4 (3.3)	3 (2.5)	9 (7.4)	2 (1.6)	0 (0)	0 (0)

†Pb2, 2nd polar body; PN, pronuclei; ‡, §, ¶, ††percentage of eggs with PN or Pb2 significantly differed between ‡ and §($P < 0.05$) and 2-cell stage significantly differed between ¶ and ††($P < 0.01$).

Table 4 Intracytoplasmic sperm injection and development of oocytes incubated in medium with and without caffeine

Medium with (+) or without (-) caffeine	Incubation time (h) injected	Number of oocytes surviving	Number of oocytes (%)	Number of eggs (%) fertilized†	Number of eggs (%) unactivated‡	Number of eggs (%) fragmented	Number of embryos developed to stage (%)		
							2-cell	Morula	Blastocyst
-	0	31	26 (83.9)	26 (100)	0 (0)	0 (0)	26 (100)	21 (80.8)	16 (61.5)
	24	31	28 (90.3)	0 (0)	22 (78.6)	6 (21.4)	0 (0)	0 (0)	0 (0)
+	24	30	29 (96.7)	11 (37.9)	12 (41.4)	6 (20.7)	6 (20.7)	0 (0)	0 (0)

†Eggs showed two pronuclei, and released a 2nd polar body; ‡eggs did not fragment and did not release a 2nd polar body.

groups kept for 6 h in medium with and without caffeine. In contrast, both the fertilization and development rates to the two-cell stage significantly differed between the 12 h-caffeine and 12 h-no-caffeine groups of zona-free embryos. No development to blastocyst was observed in any 12 h or 24 h group, regardless of caffeine addition.

Table 4 shows the results of ICSI and the preimplantation development of oocytes kept for 24 h in medium with or without caffeine. The fertilization rate in the caffeine group (38%) was significantly lower than that in the 0 h-group (100%). Although the caffeine group had a higher fertilization rate than the no-caffeine group (0%), the two-cell stage embryos of the caffeine group showed no further development.

DISCUSSION

IN THIS STUDY, using IVF and ICSI examination methods, we examined the fertilization and preimplantation development abilities of oocytes incubated with caffeine for a prolonged period.

In IVF, the 6 h-caffeine and 6 h-no-caffeine groups showed similar fertilization rates, indicating that the oocytes in both groups had identical fertilizability. The fertilization rate of 12 h-caffeine oocytes was higher than that of 12 h-no-caffeine group, but further development beyond two-cell stage was poor. The percentage of morphologically normal oocytes in the 24 h-caffeine group was similar to that in the non-kept (0 h) group. The fertilization rates of these oocytes were lower than that in the 0 h-group, indicating identical morphology, although the quality was quite different. After accounting for the age-related changes observed in zonae pellucidae and plasmalemmae by ICSI, the percentage of fertilized eggs in the 24 h-caffeine group was higher than that in the 24 h-no-caffeine group, although their embryonic development was poor.

Within the cytoplasm, Cdc2 and cyclin B associate with microtubules and centrosomes, particularly during late interphase and M phase.[23-25] Observations of locally regulated microtubule dynamics in maturing starfish oocytes[26] and in mitotic ctenophore eggs[27] indicate that regionalized MPF activation occurs in relation to nuclear/spindle position. Nuclei and microtubule asters have independent but additive effects on MPF activation, and cooperate to trigger MPF activation within the egg.[28] Although MPF can be activated in the absence of nuclei, centrosomes and microtubules in *Xenopus* eggs, these structural components are not merely effectors but are active protagonists in controlling cell cycle progression.[28]

Mitotic spindles determine the site of cleavage.[29] The positions of microtubule asters also determine the location for formation of the cleavage furrow.[30,31] Microtubule asters signal the cell cortex to initiate a cleavage furrow, for which actin filament organization is involved. Depolymerization of actin filament inhibits both cleavage and cytofragmentation.[32]

The IVF experiments carried out in our study revealed no significant difference in the zona-intact oocytes between caffeine and no-caffeine treatments, suggesting that caffeine has no discernible effect on zonae pellucidae and plasmalemmae.

Our results suggest that disruption of the meiotic spindle and disorganization of the actin filament might be responsible for the poor preimplantation development. Disruption in the cytoskeleton might be responsible for the abnormal shapes of embryos derived from oocytes treated with caffeine. Spindle disruption does not cause cytofragmentation, but does induce cell cycle arrest during mitosis.[32] Therefore, in our parthenogenetic activation experiments and ICSI experiments, 17% and 41% of the eggs, respectively, remained at the one-cell stage without fragmentation, possibly due to a defect in the entry to mitosis.

Kikuchi *et al.*[14] added caffeine to the culture medium of aged oocytes, which have a high pre-MPF level, whereas we added caffeine to the medium of non-aged

oocytes. In our experiments, we did not determine the exact time when the MPF level became low or when the caffeine elevated the MPF level in the caffeine-treated oocytes. Future study should include measurement of the MPF level and examination of chromosomes and cytoskeletal filaments in oocytes and embryos treated with caffeine.

ACKNOWLEDGMENTS

WE THANK DR S. Miyamoto and Dr Y. Hirose of Tsukuba Primate Center for their technical support. This study was supported in part by a grant from the Ministry of Health, Labour and Welfare of Japan, and by special coordination funds for the Promotion of Science and Technology.

REFERENCES

[1] Yanagimachi R. Mammalian fertilization. In: Knobil E, Neil J, Ewing LL, Greenwald GS, Markert CL, Pfaff DW, eds. *The Physiology of Reproduction*. New York: Raven Press, 1988; **1**: 135–185.

[2] Ozil JP. The parthenogenetic development of rabbit oocytes after repetitive pulsatile electrical stimulation. *Development* 1990; **109**: 117–127.

[3] Masui Y, Markert CL. Cytoplasmic control of nuclear behavior during meiotic maturation of frog oocytes. *J Exp Zool* 1971; **177**: 129–146.

[4] Smith LD, Ecker RE. Regulatory processes in the maturation and early cleavage of amphibian eggs. *Curr Top Dev Biol* 1971; **5**: 1–38.

[5] Hashimoto N, Kishimoto T. Regulation of meiotic metaphase by a cytoplasmic maturation promoting factor during mouse oocyte maturation. *Dev Biol* 1988; **126**: 242–252.

[6] Lohka MJ, Hayes MK, Maller JL. Purification of maturation promoting factor, an intracellular regulator of early mitotic events. *Proc Natl Acad Sci USA* 1988; **85**: 3009–3013.

[7] Gautier J, Minshull J, Lohka M, Glotzer M, Hunt T, Maller JL. Cyclin is a component of maturation promoting factor from *Xenopus*. *Cell* 1990; **60**: 487–494.

[8] Murray AW. Creative blocks: cell cycle checkpoints and feedback controls. *Nature* 1992; **359**: 599–604.

[9] Chian RC, Nakahara H, Niwa K, Funahashi H. Fertilization and early cleavage *in vitro* of ageing bovine oocytes after maturation in culture. *Theriogenology* 1992; **37**: 665–672.

[10] Sato E, Iritani A, Nishikawa Y. 'Formation of nucleus' and 'cleavage' of pig follicular oocytes cultured in vitro. *Jpn J Anim Reprod* 1979; **25**: 95–99.

[11] Nagai T. Parthenogenetic activation of cattle follicular oocytes *in vitro* with ethanol. *Gamete Res* 1987; **16**: 243–249.

[12] Kikuchi K, Izaike Y, Noguchi J *et al.* Decrease of histone H1 kinase activity in relation to parthenogenetic activation of pig follicular oocytes matured and aged *in vitro*. *J Reprod Fertil* 1995; **105**: 325–330.

[13] Taieb R, Thibier C, Jessus C. On cyclins, oocytes, and eggs. *Mol Reprod Dev* 1997; **48**: 397–411.

[14] Kikuchi K, Naito K, Noguchi J *et al.* Maturation/M-phase promoting factor: a regulator of aging in porcine oocytes. *Biol Reprod* 2000; **63**: 715–722.

[15] Steinmann KE, Belinsky GS, Lee D, Schlegel R. Chemically induced premature mitosis. differential response in rodent and human cells and the relationship to cyclin B synthesis and p34cdc2/cyclin B complex formation. *Proc Natl Acad Sci USA* 1991; **88**: 6843–6847.

[16] Poon RY, Chau MS, Yamashita K, Hunter T. The role of Cdc2 feedback loop control in the DNA damage checkpoint in mammalian cells. *Cancer Res* 1997; **57**: 5168–5178.

[17] Smythe C, Newport JW. Coupling of mitosis to the completion of S phase in Xenopus occurs via modulation of the tyrosine kinase that phosphorylates p34cdc2. *Cell* 1992; **68**: 787–797.

[18] Longo FJ. Changes in the zonae pellucidae and plasmalemma of aging mouse eggs. *Biol Reprod* 1981; **25**: 399–411.

[19] Toyoda Y, Yokoyama M, Hosi T. Studies on the fertilization of mouse eggs *in vitro*. I. *In vitro* fertilization of eggs by fresh epididymal sperm. *Jpn J Anim Reprod* 1971; **16**: 147–151.

[20] Whitten WK. Nutritional requirements for the culture of preimplantation embryos *in vitro*. *Adv Biosci* 1971; **6**: 129–139.

[21] Naito K, Toyoda Y, Yanagimachi R. Production of normal mice from oocytes fertilized and developed without zonae pellucidae. *Hum Reprod* 1992; **7**: 281–285.

[22] Ogonuki N, Sankai T, Yagami K *et al.* Activity of a sperm-borne oocyte-activating factor in spermatozoa and spermatogenic cells from cynomolgus monkeys and its localization after oocyte activation. *Biol Reprod* 2001; **65**: 351–357.

[23] Bailly E, Doree M, Nurse P, Bornens M. p34cdc2 is located in both nucleus and cytoplasm; part is centrosomally associated at G2/M and enters vesicles at anaphase. *EMBO J* 1989; **8**: 3985–3995.

[24] Alfa CE, Ducommun B, Beach D, Hyams JS. Distinct nuclear and spindle pole body population of cyclin-cdc2 in fission yeast. *Nature* 1990; **347**: 680–682.

[25] Ookata K, Hisanaga S, Bulinski JC *et al.* Cyclin B interaction with microtubule-associated protein 4 (MAP4) targets p34cdc2 kinase to microtubules and is a potential regulator of M-phase microtubule dynamics. *J Cell Biol* 1995; **128**: 849–862.

[26] Barakat H, Geneviere-Garrigues AM, Schatt P, Picard P. Subcellular distribution of aster-nucleated microtubule length: a more or less mitotic status of cytoplasmic areas during meiosis I of starfish oocytes. *Biol Cell* 1994; **81**: 205–213.

[27] Houliston E, Carre D, Johnston JA, Sardet C. Axis establishment and microtubule-mediated waves prior to first cleavage in *Beroe ovata*. *Development* 1993; **117**: 75–87.

[28] Perez-Mongiovi D, Beckhelling C, Chang P, Ford CC, Houliston E. Nuclei and microtubule asters stimulate maturation/M phase promoting factor (MPF) activation in

Xenopus eggs and egg cytoplasmic extracts. *J Cell Biol* 2000; 150: 963–974.

[29] Inoue S. Cell division and the mitotic spindle. *J Cell Biol* 1981; 91 (3pt; 2): 131s–147s.

[30] Rappaport R. Establishment of the mechanism of cytokinesis in animal cells. *Int Rev Cytol* 1986; 105: 245–278.

[31] Sanger JM, Dome JS, Sanger JW. Unusual cleavage furrows in vertebrate tissue culture cells. insights into the mechanisms of cytokinesis. *Cell Motil Cytoskel* 1998; 39: 95–106.

[32] Liu L, Trimarchi JR, Smith PJ, Keefe DL. Checkpoint for DNA integrity at the first mitosis after oocyte activation. *Mol Reprod Dev* 2002; 62: 277–288.

BIOLOGY OF REPRODUCTION 71, 2022–2028 (2004)
Published online before print 18 August 2004.
DOI 10.1095/biolreprod.104.031542

Cytoplasmic Asters Are Required for Progression Past the First Cell Cycle in Cloned Mouse Embryos[1]

Hiromi Miki,[3,4] Kimiko Inoue,[3] Narumi Ogonuki,[3] Keiji Mochida,[3] Hiroshi Nagashima,[5] Tadashi Baba,[4] and Atsuo Ogura[2,3]

RIKEN Bioresource Center,[3] Koyadai, Tsukuba, Ibaraki 305-0074, Japan
Graduate School of Life and Environmental Sciences,[4] University of Tsukuba, Tsukuba, Ibaraki 305-8572, Japan
Meiji University Graduate School,[5] Kawasaki, Kanagawa 214-8571, Japan

ABSTRACT

Unlike the oocytes of most other animal species, unfertilized murine oocytes contain cytoplasmic asters, which act as microtubule-organizing centers following fertilization. This study examined the role of asters during the first cell cycle of mouse nuclear transfer (NT) embryos. NT was performed by intracytoplasmic injection of cumulus cells. Cytoplasmic asters were localized by staining with an anti-α-tubulin antibody. Enucleation of MII oocytes caused no significant change in the number of cytoplasmic asters. The number of asters decreased after transfer of the donor nuclei into these enucleated oocytes, probably because some of the asters participated in the formation of the spindle that anchors the donor chromosomes. The cytoplasmic asters became undetectable within 2 h of oocyte activation, irrespective of the presence or absence of the donor chromosomes. After the standard NT protocol, a spindle-like structure persisted between the pseudopronuclei of these oocytes throughout the pronuclear stage. The asters reappeared shortly before the first mitosis and formed the mitotic spindle. When the donor nucleus was transferred into preactivated oocytes (delayed NT) that were devoid of free asters, the microtubules and microfilaments were distributed irregularly in the ooplasm and formed dense bundles within the cytoplasm. Thereafter, all of the delayed NT oocytes underwent fragmentation and arrested development. Treatment of these delayed NT oocytes with Taxol, which is a microtubule-assembling agent, resulted in the formation of several aster-like structures and reduced fragmentation. Some Taxol-treated oocytes completed the first cell cycle and developed further. This study demonstrates that cytoplasmic asters play a crucial role during the first cell cycle of murine NT embryos. Therefore, in mouse NT, the use of MII oocytes as recipients is essential, not only for chromatin reprogramming as previously reported, but also for normal cytoskeletal organization in reconstructed oocytes.

developmental biology, early development, embryo, gamete biology, ovum

INTRODUCTION

Although somatic cell cloning has been performed successfully in several mammalian species, it has emerged from recent studies that the biological factors and technical issues that affect the efficiency of cloning differ from species to species. For example, the timing of nuclear transfer (NT) and oocyte activation has a major impact on the outcome of the cloning procedure. In livestock (cattle, sheep, swine, and goats) animals, this timing seems to be relatively flexible as compared with mice. In goats and sheep, preactivated oocytes have been used for NT, leading to the production of normal offspring [1, 2]. In cattle, although the use of MII oocytes as recipients is known to support the optimal in vitro development of reconstructed embryos, at least some of the embryos that are derived from preactivated oocytes undergo preimplantation development [3]. In contrast, in mice the use of MII oocytes is critical for reconstructed embryos to complete the first cell cycle [4]. Even oocytes that receive the donor nucleus 1–2 h after activation inevitably arrest their development during the S phase of the pronuclear stage and undergo severe fragmentation [5]. This is one of the major obstacles to mouse cloning, since murine oocytes may be activated accidentally during handling in vitro (e.g., during enucleation) before NT. Previously, it has been demonstrated that the use of MII oocytes in NT is critical for the transferred donor nuclei to be able to reprogram their chromatin structures and initiate zygotic gene activation (ZGA) according to the normal schedule [6]. However, the major round of ZGA occurs during the second cell cycle (two-cell stage) in the mouse [7], which makes it very unlikely that incomplete genomic reprogramming causes the severe fragmentation seen in delayed NT oocytes during the first cell cycle.

In unfertilized murine oocytes, the microtubule-organizing centers (MTOCs), which comprise the so-called cytoplasmic asters (cytoasters), play central roles in the apposition of the male and female pronuclei and in centrosomal inheritance of cleavage stage–embryos [8]. In most animals other than the mouse, the centrosomes are inherited mainly from the fertilizing spermatozoa, from which the MTOC is organized (reviewed in [9]). Therefore, it is possible that the interactions that occur between microtubules and chromosomes during the reconstruction and first cell cycle of cloned embryos differ between mice and other animals. The present study was undertaken to determine 1) the roles of cytoplasmic asters during the first cell cycle of cloned murine embryos; and 2) the effects of NT timing on aster behavior, which may be related to the embryo fragmentation that is observed specifically in delayed NT murine oocytes.

MATERIALS AND METHODS

Culture Media

The oocytes were cultured in bicarbonate-buffered potassium simplex optimized medium (KSOM) that was supplemented with 0.1 mg/ml poly-

[1]Supported by grants from MEXT, MHWL, and the Human Foundation, Japan.
[2]Correspondence: A. Ogura, RIKEN Bioresource Center, 3-1-1, Koyadai, Tsukuba, Ibaraki 305-0074, Japan. FAX: 81 29 836 9172; e-mail: ogura@rtc.riken.go.jp

Received: 1 May 2004.
First decision: 4 June 2004.
Accepted: 11 August 2004.

ISSN: 0006-3363. http://www.biolreprod.org

vinyl alcohol and 3 mg/ml bovine serum albumin (BSA) [10]. Drops of the culture medium were covered with mineral oil (Nacalai, Tokyo, Japan) and maintained under 5% CO_2 in air at 37°C. Oocyte handling and micromanipulation were carried out in BSA-free Hepes-buffered KSOM medium (Hepes-KSOM; pH 7.4) in air.

Preparation of Oocytes and Cumulus Cells

B6D2F1(C57BL/6 × DBA/2) female mice (SLC, Shizuoka, Japan), 8–12 weeks of age, were used for the collection of recipient oocytes and donor cumulus cells. The mice were superovulated by the injection of 7.5 IU eCG, followed by 7.5 IU hCG about 48 h later. Oocytes were collected from the oviducts about 15 h after hCG injection and released from the cumulus cells by treatment with 0.1% bovine testicular hyaluronidase in KSOM medium. These oocytes and cumulus cells were incubated in KSOM until use. All procedures described within were reviewed and approved by the Animal Experimental Committee at the RIKEN Institute and were performed in accordance with the Guiding Principles for the Care and Use of Laboratory Animals.

Nuclear Transfer and Oocyte Activation

Nuclear transfer and oocyte activation were carried out according to the method reported previously [11, 12]. The timing of NT and oocyte activation differed according to the experimental groups, as described below. The recipient MII oocytes were enucleated, together with a small amount of the surrounding cytoplasm in Hepes-buffered KSOM that contained 7.5 μg/ml cytochalasin B (Calbiochem, Darmstadt, Germany) on a heated manipulation stage (37°C). Enucleation was performed using a Piezo-driven micromanipulator (Prime Tech, Ibaraki, Japan). The oocytes were allowed to regenerate their membranes in KSOM medium for 1–2 h. For NT, the cumulus cells were placed in 6% polyvinylpyrrolidone solution, and their nuclei were injected into enucleated oocytes in Hepes-buffered KSOM at room temperature using the Piezo-driven micromanipulator. The oocytes were activated by treatment with 3 mM $SrCl_2$ in Ca^{2+}-free KSOM medium for 1 h. When NT was carried out before oocyte activation (standard protocol, Group A), the oocytes were cultured for an additional 5 h in the presence of 5 μg/ml cytochalasin B to prevent the extrusion of a polar body that contained some of the donor chromosomes.

Experimental Design

This study involved five experimental groups (Fig. 1): Group A, standard NT protocol, in which the oocytes were activated 2 h after NT; Group B, simultaneous NT, in which the oocytes were activated within 5 min after NT; Group C, delayed NT, whereby NT was performed 2 h after activation; Group D, diploid parthenotes, in which the oocytes were activated without enucleation and NT; and Group E, enucleated oocytes, whereby the oocytes were enucleated and activated without NT. The distribution patterns of the microtubules, microfilaments, and chromosomes were observed at 2, 8–12, and 15 h after activation using the indirect immunofluorescence method described below.

Some of the delayed NT oocytes were treated with Taxol, which promotes microtubule assembly, to investigate whether microtubule network reformation improved the abnormal cellular kinetics of delayed NT oocytes. In a preliminary experiment using parthenogenetic embryos, we found that Taxol treatment itself induced abnormal, uneven cleavage or mild fragmentation (consisting of two to eight fragments) of embryos. Therefore, we employed two protocols in which embryos were subjected to long- or short-term exposure to Taxol-containing medium. In the first protocol, enucleated oocytes were activated for 1 h with $SrCl_2$ in Ca^{2+}-free KSOM medium that contained 1.5 μM Taxol. After 1 h of treatment with Taxol in normal KSOM medium and nuclear transfer, the reconstructed oocytes were treated with Taxol for a further 1–2 h (total of 3–4 h exposure to Taxol). In the second protocol, delayed NT oocytes, which were prepared as described above (Group C), were exposed to 0.2 μM Taxol for only 10 min after nuclear transfer. In both protocols, the reconstructed oocytes were cultured in Taxol-free KSOM for 72 h, and their developmental stages were recorded.

Immunofluorescence Staining

Oocytes were fixed and immunostained for microtubules, microfilaments, and DNA using a modification of the method described by Navara et al. [9]. Briefly, zona pellucidae were removed with acidified M2 medium (pH 2.5) at 37°C. After a 30-min period of recovery at 37°C, the zona-free oocytes were attached to MAS-coated slide glasses (Matsunami

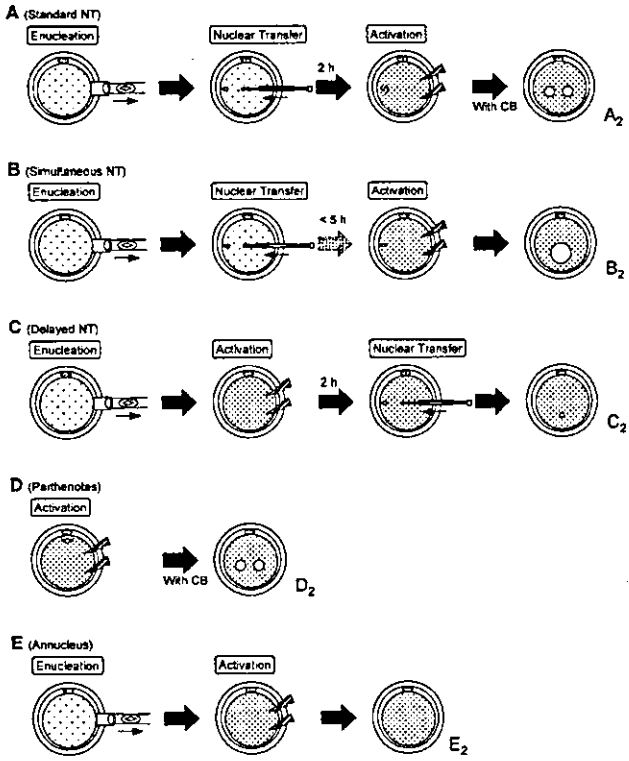

FIG. 1. Scheme showing the experimental groups. Nuclear transfer was undertaken with three different time schedules (Groups A–C). Groups D and E are non-NT groups. The characters A_2–E_2 correspond to those used in Figure 3.

Glass, Tokyo, Japan) and extracted for 2–3 min with buffer M (25% [v/v] glycerol, 50 mM KCl, 0.5 mM $MgCl_2$, 0.1 mM EDTA, 1 mM EGTA, 50 mM imidazole hydrochloride, and 1 mM 2-mercaptoethanol; pH 6.8) that contained 0.01%–0.2% Triton X-100. The permeabilized oocytes were transferred to dry slide glasses and fixed in 3% formaldehyde for 20 min at room temperature. Permeabilization and fixation were performed at 37°C to maintain the original microtubule configuration. Fixed oocytes were then blocked overnight with 0.1 M PBS that contained 0.1% Triton X-100 and 3 mg/ml BSA (PBS-TX-BSA) at 4°C. The oocytes were incubated with a murine monoclonal antibody against α-tubulin (clone DM 1A, diluted 1:500; Sigma Chemical Co., St. Louis, MO) for 40 min at 37°C. After washing in PBS-TX-BSA, the samples were stained with FITC-conjugated goat anti-mouse IgG antibody (diluted 1:100; Sigma). They were then nuclear stained for DNA with DAPI (4,6-diamidino-2-phenylindole) or propidium iodide. For the staining of actin filaments, the oocytes were cultured with rhodamine-conjugated phalloidin (50 μg/ml; Sigma) before DNA staining. The slide glasses were mounted in antifade medium (Vectashield; Vector Labs, Burlingame, CA) and examined using a TE2000 epifluorescence microscope (Nikon, Tokyo, Japan).

RESULTS

In this study, 5–30 oocytes were observed immunohistochemically for each group at each time point. The results from at least two replicate experiments are summarized. The localization patterns of the microtubules and chromosomes were essentially the same within a set of oocytes, except for those observed at 8–12 h in Groups C and E, which consisted of various misshapen forms before fragmentation.

Behavior of Cytoplasmic Asters in Nuclear-transferred MII Oocytes

We examined the behavioral patterns of the cytoplasmic asters in MII-arrested oocytes, both before and after NT.

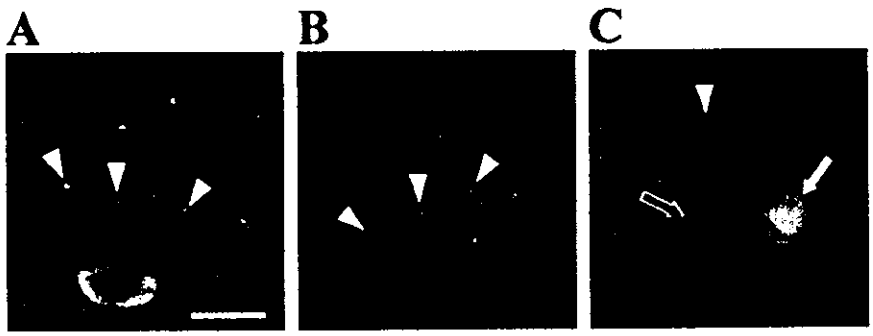

FIG. 2. Cytoplasmic asters in MII oocytes before and after NT. A) Intact MII oocytes, which contain an average of approximately 15 asters per oocyte (arrowheads; see text for details). B) MII oocytes after enucleation. No change is found in the number or distribution of asters (arrowheads) as compared with intact oocytes. C) Enucleated oocytes 1 h after NT. The number of cytoplasmic asters (arrowhead) is decreased significantly, whereas a newly formed spindle encloses the condensed donor chromosomes (white arrow). The area proximal to the spindle contains fewer asters (black arrow) than the area distal to the spindle. Bar = 20 μm.

Removal of the meiotic spindles from MII oocytes did not change the number or distribution of cytoplasmic asters (14.9 ± 3.0 vs. 15.1 ± 3.8 (mean ± SD asters per oocyte; $P > 0.05$; Fig. 2, A and B). However, 1–2 h after transfer of the donor nucleus, the number of cytoplasmic asters decreased significantly (8.9 ± 2.9; $P < 0.01$), whereas a newly formed spindle enclosed the condensed donor chromosomes (Fig. 2C). The area proximal to the spindle had fewer asters than the area distal to the spindle (Fig. 2C). These findings suggest that cytoplasmic asters participate in the reformation of the metaphase spindle that anchors the donor chromosomes.

Behavior of Microtubules in Nuclear-transferred Oocytes After Activation

To gain a better understanding of the postactivation behavior of microtubules in nuclear-transferred oocytes, we observed the temporal and spatial changes in microtubule distribution in the oocytes from three groups with different NT and activation timings (see Fig. 1 for experimental design). At 1–2 h after activation (Fig. 3, A_1, B_1, and C_1), the oocytes proceeded to the anaphase-telophase transition. At this stage, cytoplasmic asters were undetectable in Groups A and C, whereas some asters were detected in Group B. Although the asters that had exhibited intense fluorescence disappeared, the fine microtubule network remained and was evenly distributed throughout the cytoplasm. Intense fluorescence for tubulin was restricted to the spindle between the segregating donor chromosomes in Group A (standard NT; Fig. $3A_1$). When the chromosomes segregated into three masses, a tridirectional spindle was formed (Fig. $3A_1$, inset). In Group B (simultaneous NT), dense bundles of microtubules (or assemblies of asters) often surrounded the introduced donor nucleus (Fig. $3B_1$).

At 8–12 h after activation (Fig. 3, A_2, B_2, and C_2), the oocytes were at the midpronuclear stage and formed two pseudopronuclei (Group A) or one large pseudonucleus (Group B). The spindle-shaped dense microtubule arrays were still found between the two pseudopronuclei in Group A. In Group C oocytes (delayed NT), the donor nucleus retained its original size or was slightly larger, and strong fluorescence was absent in the cytoplasm or around the nucleus. The fine microtubule network was present in the cytoplasm, although its distribution was very irregular. Many of these delayed NT oocytes had bumpy surfaces and showed irregular distributions of microfilaments and microtubules within the ooplasm (Fig. 4B). This finding is in marked contrast to the observations of oocytes from Group A, in which the microfilaments were evenly distributed only on the surface area of the cortex (Fig. 4A).

At 15 h after activation (Fig. 3, A_3 and B_3), most of the oocytes in Groups A and B entered the prometaphase or metaphase, as evidenced by nuclear membrane breakdown. All of the oocytes in Group C showed complete fragmentation at this stage (see also Fig. 5). During the early prometaphase, the condensing chromosomes were surrounded by dense microtubule arrays without nucleation sites, whereas several asters reappeared in the cytoplasm (Fig. $3A_3$). As this stage proceeded, the asters migrated to the condensed chromosomes and gradually formed the mitotic spindle. This type of microtubule behavior was common to Groups A and B.

In the non-NT oocytes (Groups D and E), the chromosomes and microtubules behaved as those in the NT groups (Groups A and C, respectively). The parthenogenetically activated oocytes in Group D (Fig. 3D) showed the same microtubule distribution pattern as those in Group A (Fig. 3A), although the chromosome composition of the (pseudo)pronuclei was different (in parthenogenetic oocytes, each pronucleus contained a haploid set of chromosomes). The oocytes in Group E were enucleated, but not nuclear-transferred (Fig. 3E). After activation, they underwent fragmentation within 15 h, in a similar fashion to the delayed NT oocytes in Group C (Fig. 3C).

In Groups A and D, the microfilament-disrupting agent cytochalasin was included in the medium for the first 6 h postactivation to prevent polar body extrusion. In preliminary experiments, we confirmed that this treatment had no significant effects on the behavioral patterns of the microtubules or cytoplasmic asters (data not shown).

TABLE 1. Effect of Taxol treatment on in vitro development of embryos reconstructed by delayed NT with cumulus cells.

	No. observed	No. (%) fragmentation	No. (%) 1-cell	No. (%) 2-cell	No. (%) 4-cell	No. (%) morula blasts.	No. (%) abnormal cleavage*
Taxol 3–4 h	110	0 (0.0)	0 (0.0)	0 (0.0)	0 (0.0)	0 (0.0)	110 (100.0)
Taxol 10 min	149	124 (83.2)	7 (4.7)	11 (7.4)	2 (1.3)	5 (3.4)	0 (0.0)
No treatment	78	78 (100.0)	0 (0.0)	0 (0.0)	0 (0.0)	0 (0.0)	0 (0.0)

* Including mild fragmentation induced by toxicity of taxol.

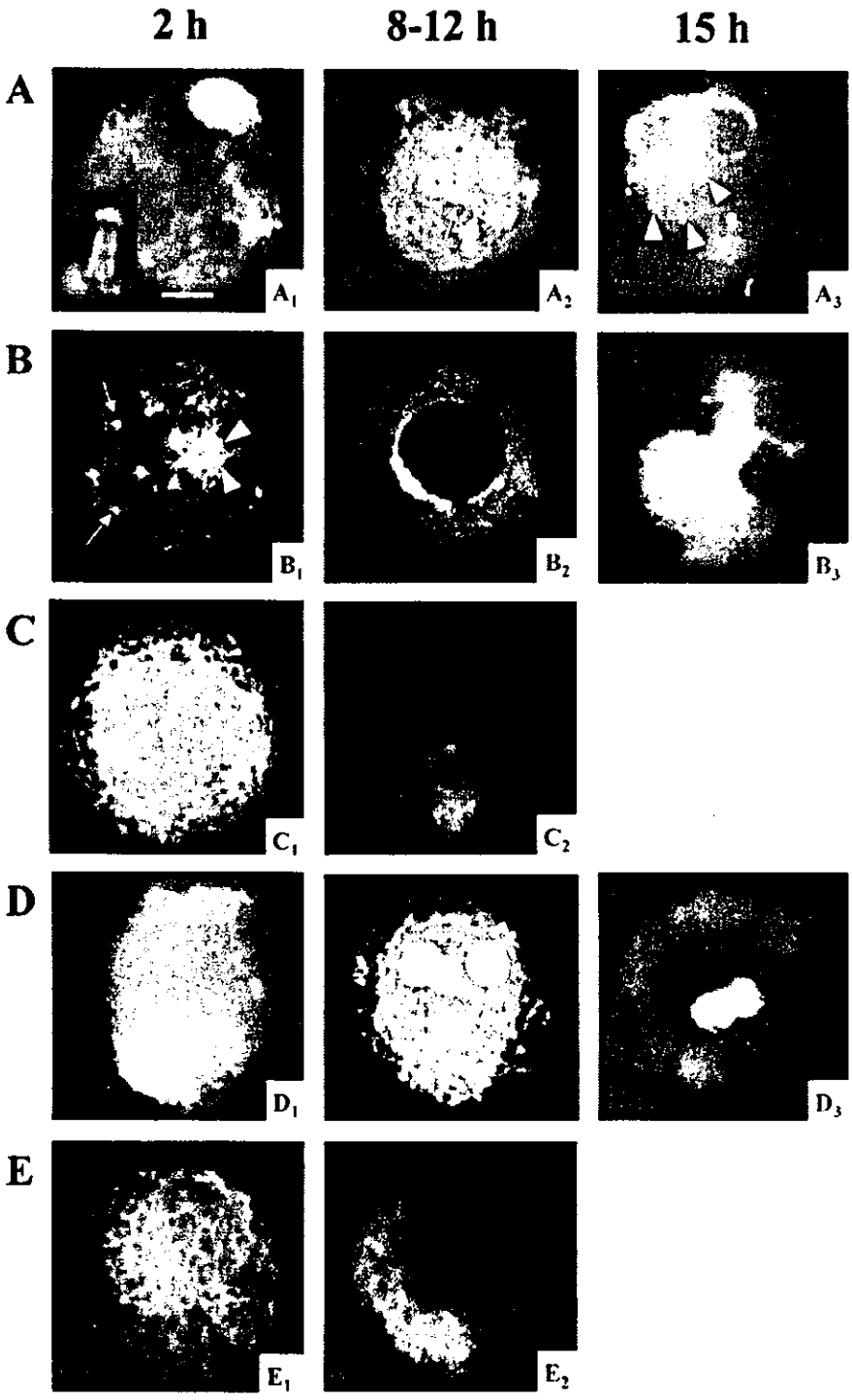

FIG. 3. Distribution of microtubules (green) and chromosomes (red or blue) in NT and parthenogenetic embryos after activation. **A**) Group A (standard NT). At 2 h after activation (A_1), the oocyte is in telophase II, and the donor chromosomes are segregated into two compact masses (red). The chromosomes rarely segregated into three masses (inset). Cytoplasmic asters are not visible. At 8–12 h (A_2) after activation, the pseudopronuclei (blue) are fully swollen. Intense staining for microtubules is seen in the remnant of the spindle (arrow), whereas a fine microtubule network is formed in the entire cytoplasm (see also Fig. 4A). At 15 h (A_3) postactivation, the nuclei show the prometaphase configuration with condensing chromosomes. Several asters (arrowheads) appear in the cytoplasm. **B**) Group B (simultaneous NT). At the stage corresponding to telophase II (2 h; B_1), the donor chromosomes are not segregated but are condensed in a single mass (red). Cytoplasmic asters persist in the cytoplasm (arrows) and around the donor nucleus (arrowheads). At 8–12 h (B_2), a large pseudopronucleus develops and asters are not present. The oocytes enter mitosis by 15 h (B_3) postactivation, as in Group A. This oocyte is already in the mitotic telophase. Microtubules are distributed mainly to the spindle and around the sister chromosomes. **C**) Group C (delayed NT). The donor nuclei are introduced into recipient oocytes 1–2 h after activation. The photo shows an enucleated oocyte before NT. It has no cytoplasmic asters (C_1). At 8–12 h (C_2), the donor nucleus retains its original size. Uneven distribution of the fine microtubule network is noted in the cytoplasm (see also Fig. 4B). By 15 h, all of the NT oocytes have undergone fragmentation (see Fig. 5C). **D**) Group D (diploid parthenote). The behavioral patterns of the microtubules and chromosomes are very similar to those in the standard NT group (**A**). The oocyte at 15 h (D_3) is in late prometaphase, showing completely condensed chromosomes (red) and dense microtubules (green) shortly before spindle formation. **E**) Group E (enucleated oocytes). The oocytes lack nuclei and have undergone fragmentation, as is seen for the oocytes in Group C. The irregular distribution pattern of fine microtubules (E_2) is very similar to that in Group C (C_2). Bar = 20 μm.

Effect of Taxol Treatment on the Behavior of Delayed NT Oocytes

The behavior of microtubules and microfilaments, as described above, indicates that cytoplasmic fragmentation in delayed NT oocytes (Group C) may be attributed to the absence of cytoplasmic asters at the time of NT. To obtain further experimental evidence to support this hypothesis, we treated recipient oocytes with Taxol, which is a microtubule-assembling agent, and examined whether the enhancement of microtubule assembly improved the cellular kinetics of these delayed NT oocytes. In the first protocol, numerous aster-like structures were found in the cytoplasm 2 h after Taxol treatment (shortly before NT), irrespective of the presence or absence of oocyte chromosomes (Fig. 5A). Taxol-treated oocytes were then reconstructed with the

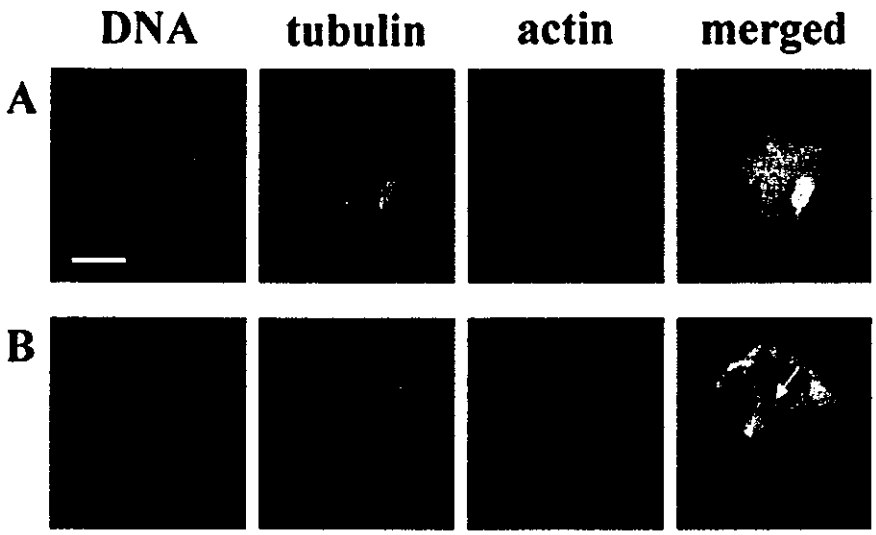

FIG. 4. Oocytes after standard NT or delayed NT, 8 h after activation. The oocytes were stained for the localization of nuclei (blue), microtubules (green), and microfilaments (red). An oocyte after standard NT in (A) has a regular round shape and shows even distributions of fine microtubules in the cytoplasm and of microfilaments in the cortex area. The arrow indicates the remnant of the spindle. In contrast, an oocyte that was subjected to delayed NT (B) has a bumpy surface and irregular distributions of microtubules and microfilaments. The dense yellow bundles in the merged photomicrograph indicate colocalization of microtubules and microfilaments in the cytoplasm (arrows). Bar = 20 μm.

donor nucleus that was produced by delayed NT and cultured for 15 h. As expected, the reconstructed oocytes did not show severe fragmentation that was specific for delayed NT, but did show uneven cleavage or mild fragmentation with two to eight karyoplasts/cytoplast (Fig. 5B). These oocytes showed arrested development thereafter (Table 1). In the second protocol, the oocytes were exposed to Taxol for only 10 min, immediately after nuclear transfer, to minimize the cytotoxic effect of Taxol. Although delayed NT-specific severe fragmentation was induced in some oocytes, the remaining oocytes (n = 25) survived the first cell cycle. Of the latter 25 oocytes, five (20%) developed to the morula/blastocyst stage (two morulae and three blastocysts; Fig. 5B, inset; Table 1). In contrast, all of the oocytes in the nontreated group underwent complete fragmentation (Fig. 5C).

DISCUSSION

It is generally accepted that the coordinated behavior of microtubules and donor chromosomes in nuclear-transferred oocytes is a prerequisite for the subsequent normal development of cloned embryos [13–15]. Murine MII oocytes contain two microtubule-containing structures: the meiotic spindles and a dozen cytoplasmic microtubules (asters). The meiotic spindles are crucial for the proper alignment and separation of the chromosomes during meiosis, whereas the cytoplasmic asters are responsible for pronuclear apposition following sperm incorporation [9]. The meiotic spindles are removed from MII oocytes before NT. In this report, we show that in the mouse, the cytoplasmic asters play key roles in pronuclear movement following oocyte activation and in donor chromosome alignment during spindle formation in recipient MII oocytes. The cytoplasmic asters in nuclear-transferred oocytes are probably assembled in the spindle poles, thereby stabilizing the spindle microtubules.

The situation described above is in sharp contrast to that pertaining to NT cloning in domestic animal species, since the MII oocytes of the latter lack cytoplasmic asters. Recent studies of microtubule configuration following somatic cell NT in cattle and pigs suggest a major contribution on the part of the donor cell centrosome (or centrosomal material, γ-tubulins) to the formation of the spindle that encloses the donor chromosomes, although newly appearing cytoplasmic asters are involved to a lesser extent [16, 17]. Interestingly, even when preactivated oocytes were used as recipients, these donor-derived centrosomes participated in the formation of spindles that were associated with the donor pronuclear-like structure and played a role in the positioning of this structure. These patterns are essentially

FIG. 5. Effect of Taxol on fragmentation induced in oocytes after delayed NT (Group C). A) Aster-like structures are formed in the cytoplasm 2 h after activation (arrows). B) Oocytes in the delayed NT group at 15 h after activation. These oocytes were treated with Taxol for 2 h before and after NT. Some of them retain normal appearance, but gradually undergo uneven cleavage (arrows) or mild fragmentation (arrowheads; compare with the severe fragmentation in C). Some of the oocytes that were treated with Taxol for 10 min after nuclear transfer cleaved and developed into blastocysts (inset). C) Oocytes in the delayed NT group without Taxol treatment. All of the oocytes have undergone complete fragmentation by 15 h after activation. Bar = 50 μm.

similar to that resulting from NT using blastomere nuclei [18]. Therefore, in domestic animal species the preactivated ooplasm that receives the donor nucleus develops through several cleavages, although very few of these ooplasts reach the blastocyst stage [3, 16]. Activated bovine oocytes that are enucleated at the telophase II stage have also proven to be suitable for NT [19], which indicates a certain amount of flexibility in the timing of NT and oocyte activation in the cloning of domestic species. In contrast, murine nuclear-transferred embryos from preactivated oocytes are never cleaved, and all of them undergo severe fragmentation during the first cell cycle [4, 5]. To date, only one cloned pup has been born from embryonic stem cells using preactivated oocytes that were chemically enucleated by demecolcine [20]. It would be interesting to know whether cytoplasmic asters persisted in these experiments, since as many as 36% of the reconstructed oocytes were cleaved [20]. An interval of 1 h between oocyte activation and NT is sufficient for fragmentation, as shown in this and previous studies [5]. Thus, murine somatic cell NT appears to be relatively inflexible in terms of the timing of oocyte activation and NT, although the reason for this is unclear.

The cytoskeletal dynamics observed during NT in this study indicate that the inability of murine preactivated oocytes to behave as appropriate recipients may be because of the lack of asters (or microtubule-nucleating activity) in the ooplasm at the time of NT. The cytoplasmic asters disappeared rapidly (within 2 h) after oocyte activation in all of the experimental groups, except for Group B, in which some asters remained for reasons unknown. Aster disappearance occurred irrespective of the presence or absence of the MII spindle (i.e., the oocytes in all the experimental groups, including the parthenogenetic group, had exactly the same pattern of aster disappearance). This phenomenon has also been noted with normally fertilized oocytes that were activated by spermatozoa [21, 22]. The disappearance of cytoplasmic asters from activated murine oocytes may reflect the loss of microtubule-nucleating activity. In the fertilized oocytes at S phase, a few γ-tubulin spots remained in the vicinity of the pronuclei, although well-developed cytoplasmic asters were not discernible.

The patterns of distribution of the fine microtubule networks in the cytoplasm, from which asters disappeared following activation, differed significantly among the experimental groups. The networks in the oocytes of the standard NT group (delayed activation) were distributed uniformly throughout the cytoplasm, whereas those in the delayed NT group showed irregular, patchy, or band distributions. The latter situation was also observed for enucleated oocytes that were activated without NT (Group E). In addition to these abnormal distributions of microtubules, we detected phalloidin-reactive actin filaments, which normally show a distinctive intense cortical band. It is known that contractile ring formation by actin filaments promotes cell division [23]. It seems unlikely that apoptosis is involved in this cascade, since there was no morphological evidence for apoptotic changes, such as nuclear splitting and chromatin aggregation, in the nuclei (data not shown). Therefore, the abnormal recruitment of actin filaments in delayed NT oocytes may lead directly to cytoplasmic fragmentation. However, the reason why abnormal distributions of microtubules and actin filaments occur in delayed NT oocytes remains unclear. To address this question, we treated delayed-NT oocytes with Taxol. This drug induces the formation of aster-like structures in activated oocytes. Therefore, the donor nucleus was introduced into oocyte cytoplasm that contained asters, as in standard NT. Interestingly, severe cytoplasmic fragmentation, which is inevitable in delayed NT oocytes, was not found in oocytes that were treated with Taxol for 3–4 h. However, Taxol induced abnormal cleavage or mild fragmentation (two to eight fragments) of oocytes, and we could not assess the developmental ability of the delayed-NT oocytes that were rescued by Taxol treatment. Therefore, in the second protocol, we treated the oocytes with Taxol for only 10 min to minimize the cytotoxicity of Taxol. As expected, fragmentation occurred in some oocytes owing to delayed NT, whereas the remaining oocytes escaped both fragmentation and Taxol toxicity and developed further. These findings clearly indicate that the presence of asters, or related microtubule nucleation activity, in the recipient ooplasm at the time of NT is crucial for the establishment of the normal nuclear-cytoskeletal configuration in nuclear-transferred oocytes. Thus, the use of MII oocytes is essential for successful mouse somatic cell cloning by NT, at least with regard to cytoskeletal dynamics.

Previously, it was reported that in the case of murine nuclear-transferred oocytes, normal chromatin reprogramming events, which include the silencing of donor nucleus transcription, the accumulation of TATA box-binding proteins, and increased DNase I sensitivity, occur only when the donor nucleus is introduced into MII-arrested recipient oocytes [6]. Chromatin reprogramming leads to zygotic gene activation at the appropriate time point after oocyte activation, and thereafter to normal embryo development. Taken together, our results and those of previous studies suggest that the use of MII oocytes as recipients in mouse cloning experiments is critical, not only for chromatin reprogramming but also for normal cytoskeletal organization in the reconstructed oocytes. This strict requirement is unique to murine somatic cell cloning.

ACKNOWLEDGMENTS

We thank Dr. Yukihiro Terada, Tohoku University, for his continued invaluable suggestions.

REFERENCES

1. Baguisi A, Behboodi E, Melican D, Pollock JS, Destrempes MM, Cammuso C, Williams JL, Nims SD, Porter CA, Midura P, Palacios MJ, Ayres SL, Denniston RS, Hayes ML, Ziomek CA, Meade HM, Godke RA, Gavin WG, Overstrom EW, Echelard Y. Production of goats by somatic nuclear transfer. Nat Biotech 1999; 17:456–461.
2. Campbell KHS, McWhir J, Ritchie WA, Wilmut I. Sheep cloned by nuclear transfer from a cultured cell line. Nature 1996; 380:64–66.
3. Tani T, Kato Y, Tsunoda Y. Direct exposure of chromosomes to non-activated ovum cytoplasm is effective for bovine somatic cell nucleus reprogramming. Biol Reprod 2001; 64:324–330.
4. Wakayama T, Perry ACF. Cloning of mice. In: Cibelli JB, Lanza R, Campbell K, West MD (eds.), Principles of Cloning. San Diego: Academic Press; 2002:301–341.
5. Wakayama T, Yanagimachi R. Effect of cytokinesis inhibitors, DMSO and the timing of oocyte activation on mouse cloning using cumulus cell nuclei. Reproduction 2001; 122:49–60.
6. Kim JM, Ogura A, Nagata M, Aoki F. Analysis of the mechanism for chromatin remodeling in embryos reconstructed by somatic nuclear transfer. Biol Reprod 2002; 67:760–766.
7. Schultz RM. Regulation of zygotic gene activation in the mouse. Bioessays 1993; 15:531–538.
8. Schatten H, Schatten G, Mazia D, Balczon R, Simerly C. Behavior of centrosomes during fertilization and cell division in mouse oocytes and sea urchin eggs. Proc Natl Acad Sci U S A 1986; 83:105–109.
9. Navara CS, Wu G-J, Simerly C, Schatten G. Mammalian model systems for exploring cytoskeletal dynamics during fertilization. Curr Topics Dev Biol 1995; 31:321–342.

10. Lawitts JA, Biggers JD. Culture of preimplantation embryos. Methods Enzymol 1993; 225:153–164.
11. Wakayama T, Perry ACF, Zuccotti M, Johnson KR, Yanagimachi R. Full-term development of mice from enucleated oocytes injected with cumulus cell nuclei. Nature 1998; 394:369–374.
12. Inoue K, Ogonuki N, Mochida K, Yamamoto Y, Takano K, Kohda T, Ishino F, Ogura A. Effects of donor cell type and genotype on the efficiency of mouse somatic cell cloning. Biol Reprod 2003; 69:1394–1400.
13. Chesne P, Adenot PG, Viglietta C, Baratte M, Boulanger L, Renard JP. Cloned rabbits produced by nuclear transfer from adult somatic cells. Nat Biotechnol 2002; 20:366–369.
14. Simerly C, Dominko T, Navara C, Payne C, Capuano S, Gosman G, Chong KY, Takahashi D, Chace C, Compton D, Hewitson L, Schatten G. Molecular correlates of primate nuclear transfer failures. Science 2003; 300:297.
15. Yin XJ, Kato Y, Tsunoda Y. Effect of enucleation procedures and maturation conditions on the development of nuclear-transferred rabbit oocytes receiving male fibroblast cells. Reproduction 2002; 124:41–47.
16. Shin M, Park S, Shim H, Kim N. Nuclear and microtubule reorganization in nuclear-transferred bovine embryos. Mol Reprod Dev 2002; 62:74–82.
17. Yin XJ, Cho SK, Park MR, Im YJ, Park JJ, Bhak JS, Kwon DN, Jun SH, Kim NH, Kim JH. Nuclear remodeling and the developmental potential of nuclear transferred porcine oocytes under delayed-activated conditions. Zygote 2003; 11:167–174.
18. Navara CS, First NL, Schatten G. Microtubule organization in the cow during fertilization, polyspermy, parthenogenesis, and nuclear transfer: the role of the sperm aster. Dev Biol 1994; 162:29–40.
19. Bordignon V, Smith LC. Telophase enucleation: an improved method to prepare recipient cytoplasts for use in bovine nuclear transfer. Mol Reprod Dev 1998; 49:29–36.
20. Gasparrini B, Gao S, Ainslie A, Fletcher J, McGarry M, Ritchie WA, Springbett AJ, Overstrom EW, Wilmut I, De Sousa PA. Cloned mice derived from embryonic stem cell karyoplasts and activated cytoplasts prepared by induced enucleation. Biol Reprod 2003; 68:1259–1266.
21. Maro B, Howlett SK, Webb M. Non-spindle microtubule organizing centers in metaphase II–arrested mouse oocytes. J Cell Biol 1985; 101:1665–1672.
22. Palacios MJ, Joshi HC, Simerly C, Schatten G. Gamma-tubulin reorganization during mouse fertilization and early development. J Cell Sci 1993; 104:383–389.
23. Cao L, Wang Y. Mechanism of the formation of contractile ring in dividing cultured animal cells. I. Recruitment of preexisting actin filaments into the cleavage furrow. J Cell Biol 1990; 110:1089–1095.

The *Sall3* locus is an epigenetic hotspot of aberrant DNA methylation associated with placentomegaly of cloned mice

Jun Ohgane[1], Teruhiko Wakayama[2,a], Sho Senda[1], Yukiko Yamazaki[2], Kimiko Inoue[3], Atsuo Ogura[3], Joel Marh[2], Satoshi Tanaka[1], Ryuzo Yanagimachi[2] and Kunio Shiota[1,*]

[1]*Cellular Biochemistry, Animal Resource Sciences/Veterinary Medical Sciences, The University of Tokyo, 1-1-1 Yayoi, Bunkyo-ku, Tokyo 113-8657, Japan*

[2]*The Institute for Biogenesis Research, Department of Anatomy and Reproductive Biology, John A. Burns School of Medicine, University of Hawaii, Honolulu, HI 96822, USA*

[3]*Bioresource Centre, Riken, 3-1-1, Koyadai, Tsukuba, 305-0074, Ibaraki, Japan*

DNA methylation controls various developmental processes by silencing, switching and stabilizing genes as well as remodeling chromatin. Among various symptoms in cloned animals, placental hypertrophy is commonly observed. We identified the *Spalt-like gene3* (*Sall3*) locus as a hypermethylated region in the placental genome of cloned mice. The *Sall3* locus has a CpG island containing a tissue-dependent differentially methylated region (T-DMR) specific to the trophoblast cell lineage. The T-DMR sequence is also conserved in the human genome at the *SALL3* locus of chromosome 18q23, which has been suggested to be involved in the 18q deletion syndrome. Intriguingly, larger placentas were more heavily methylated at the *Sall3* locus in cloned mice. This epigenetic error was found in all cloned mice examined regardless of sex, mouse strain and the type of donor cells. In contrast, the placentas of *in vitro* fertilized (IVF) and intracytoplasmic sperm injected (ICSI) mice did not show such hypermethylation, suggesting that aberrant hypermethylation at the *Sall3* locus is associated with abnormal placental development caused by nuclear transfer of somatic cells. We concluded that the *Sall3* locus is the area with frequent epigenetic errors in cloned mice. These data suggest that there exists at least genetic locus that is highly susceptible to epigenetic error caused by nuclear transfer.

Introduction

Most cells of higher eukaryotes differentiate without changing DNA sequence. Cells differentiate into specific types by activation and inactivation of particular sets of genes. DNA methylation is involved in various biological phenomena (Bird 2002; Li 2002) such as cell differentiation (Takizawa *et al.* 2001), X chromosome inactivation (Norris *et al.* 1991), genomic imprinting (Stoger *et al.* 1993), heterochromatin formation (Jones *et al.* 1998) and tumorgenesis (Issa *et al.* 1994).

Mammalian cloning using adult somatic cells has been successful in several species (Renard *et al.* 2002; Wilmut *et al.* 2002). Cloned offspring develop a variety of abnormal phenotypes such as increased body weight (large fetus syndrome), pulmonary hypertension, placental overgrowth, respiratory problems and early death (Lanza *et al.* 2000; Hill *et al.* 2000; Tamashiro *et al.* 2000; Tanaka *et al.* 2001; Ogonuki *et al.* 2002). This suggests a disruption of the normal developmental program. On this basis we expected and have identified several aberrantly methylated loci in the tissues of full-term cloned fetuses (Ohgane *et al.* 2001). Interestingly, each cloned animal has a different DNA methylation pattern and the extent of hyper- or hypo-methylation varies among the individuals. Cloned embryos at blastocyst or earlier developmental stages were reported to have unusual DNA methylation patterns at both repetitive and single copy gene regions (Santos *et al.* 2002; Bourc'his *et al.* 2001; Kang *et al.* 2001, 2002). Cloned fetuses of later developmental stages also showed aberrant DNA methylation at loci of imprinted and X-chromosomal genes compared with control fetuses (Humpherys *et al.* 2001; Xue *et al.*

Communicated by: Shinichi Aizawa

**Correspondence*: E-mail: ashiota@mail.ecc.u-tokyo.ac.jp

[a]Present address: Center for Developmental Biology, RIKEN, 2-2-3 Minatojima-minamimachi, Chuo-Ku, Kobe 650-0047, Japan.

DOI: 10.1111/j.1365-2443.2004.00720.x

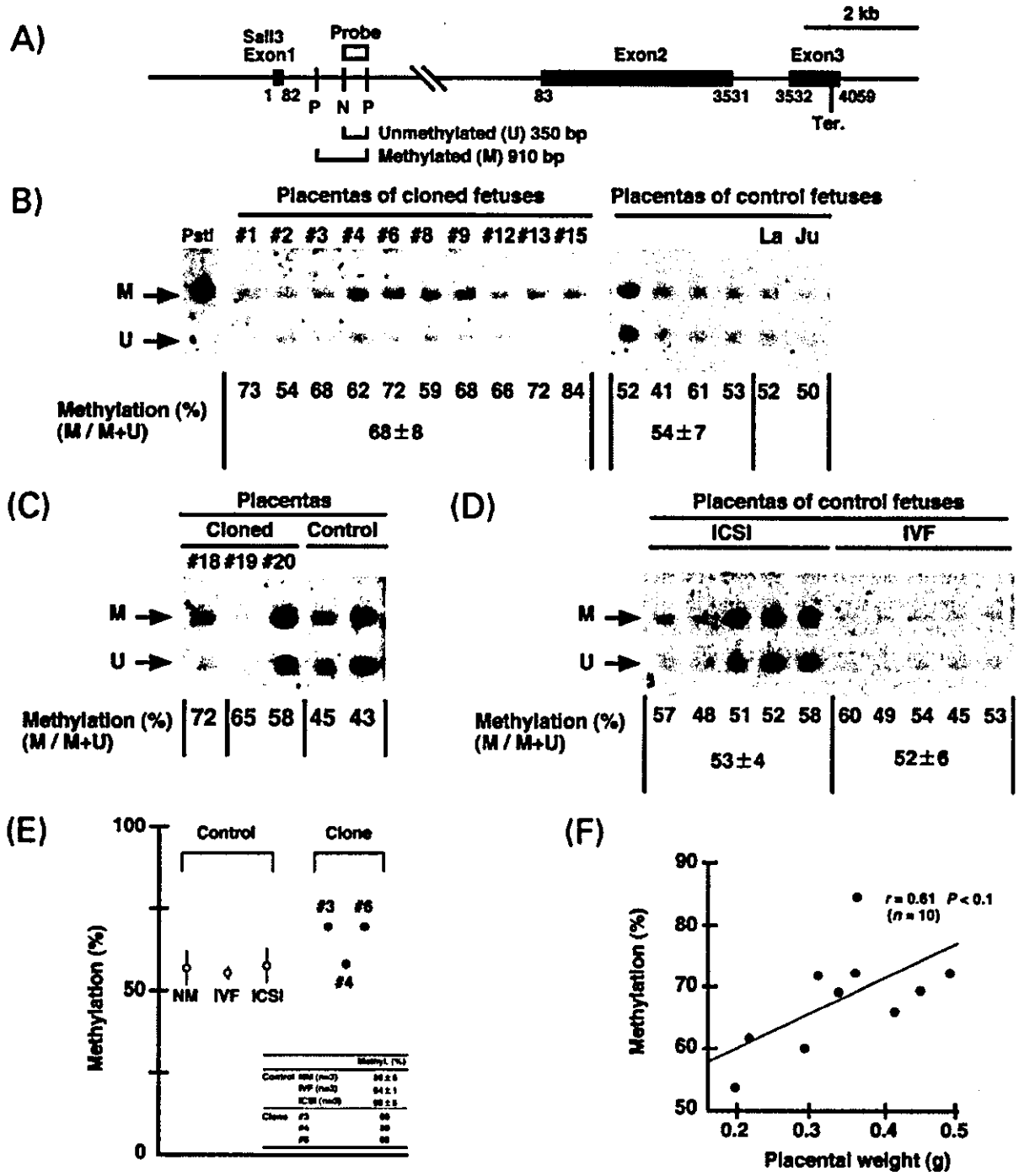

Figure 1 Aberrant DNA hypermethylation at the *Sall3* locus in placentas of cloned mice. (A) The genomic structure of the *Sall3* locus with the position of the probe and expected bands in Southern blotting. The *Sall3* locus is at the telomeric E3 subregion of chromosome 18. *Not*I is a methylation-sensitive restriction enzyme. The *Not*I site, aberrantly methylated in the placenta of the cloned mouse, is located approximately 1.1 kb downstream of *Sall3* exon 1. Closed boxes represent three exons of the *Sall3* gene. Numbers below the boxes are nucleotide numbers, designating the translation-starting site as number 1. An open box indicates the position of the probe. Methylation status of the *Sall3* locus was analysed by Southern blotting using *Not*I and *Pst*I. The bands expected in Southern blotting in Figs 1 and 3

2002). These findings suggest that cloned animals produced by somatic nuclear transfer have different methylation patterns from normal animals. At present, however, it remains to be seen whether aberrant DNA methylation at certain loci is related to the phenotypes specific to cloned animals.

Overgrowth of the placenta is one of the commonly observed symptoms in all cloned mice regardless of the sex and strain of animal and the type of donor cell (Wakayama & Yanagimachi 2001; Ogura *et al.* 2000a). Abnormal gene expression has been detected in term placentas of cloned mice (Humpherys *et al.* 2002; Suemizu *et al.* 2003). Thus, there may be genomic loci associated with the abnormal placental development in cloned mice. By using restriction landmark genomic scanning (RLGS) method, we have previously investigated genome-wide DNA methylation of CpG islands in mouse embryonic stem (ES) cells, embryonic germ (EG) cells and trophoblast stem (TS) cells before and after differentiation (Shiota *et al.* 2002). We have also investigated CpG islands of terminally differentiated germ cells and several somatic tissues using the same technique. There are many CpG islands with tissue-dependent differentially methylated regions (T-DMRs) (Imamura *et al.* 2001; Shiota *et al.* 2002). Here, we report that a T-DMR within the *Sall3* locus at the telomeric E3 subregion of mouse chromosome 18 is hypermethylated in the placentas of all cloned mice examined.

Results

Hypermethylation of the Sall3 locus in placentas of cloned mice

Based on our previous studies, we prepared a T-DMR panel consisting of 247 loci detected by RLGS, one of which, locus #148, was methylated only in TS cells (Shiota *et al.* 2002). Intriguingly, locus #148 was matched to one of the aberrantly methylated loci in the placenta of cloned mice reported in the previous paper (spot 8 in Ohgane *et al.* 2001). It is also mapped to the *Sall3* locus at the telomeric E3 subregion of mouse chromosome 18 (Fig. 1A).

We first used fetuses cloned with adult cumulus cells of B6D2F1 mice (Fig. 1B). The degree of methylation at the *Sall3* locus was 54 ± 7% in the naturally mated controls (NM) as deduced from the previous report (Ohgane *et al.* 2001; Shiota *et al.* 2002). Placentas of all 10 cloned fetuses, with the exceptions of #2 and #8, showed over 60% methylation (average 68 ± 8%). Clone #15 showed the highest DNA methylation (84%). These facts indicated that the *Sall3* locus is commonly hypermethylated in these clones. In other words, cloning by somatic cell nuclear transfer may consistently result in the epigenetic error at this specific locus of the placental genome.

Mouse placenta consists of junctional and labyrinth zones (Cross *et al.* 1994). Morphological examination of placentas revealed that an expanded spongiotrophoblast layer in the junctional zone is the major cause of placentomegaly in cloned mice (Tanaka *et al.* 2001). DNA methylation of the *Sall3* locus was not different between the labyrinth and junctional zones (52% and 50%, respectively) (Fig. 1B). This implies that the hypermethylation of the *Sall3* locus is not the result of change in the proportion of certain trophoblast subtypes in the placentas of cloned mice.

Methylation status of the Sall3 locus in placentas of cloned mice with various donor cells

Since placentomegaly is observed regardless of the types of donor cell, we next investigated whether DNA

are depicted as unmethylated (U, 350 bp) or methylated (M, 910 bp). N, *Not*I; P, *Pst*I. (B) Aberrant hypermethylation of the *Sall3* locus in placentas of fetuses cloned with female cumulus cells of B6D2F1 mice. The methylation status of placentas of cloned fetuses (n = 10) was compared with that of placentas of control B6D2F1 fetuses produced by natural mating of C57BL/6 and DBA2 mice (NM, n = 4). The value (%) under each lane denotes the methylation rate of the *Not*I site (M/M +U). The difference in methylation rate was statistically significant between the cloned and control mice (68 ± 8% and 54 ± 7%, respectively, $P < 0.01$). A NM placenta of B6D2F1 mouse was dissected into the labyrinth zone (La) and the junctional zone (Ju), and their methylation status at the *Sall3* locus was analysed. The placental labyrinth zone and the junctional zone were methylated at almost the same rates (52% and 50%, respectively). (C) Aberrant hypermethylation of the *Sall3* locus in the placentas of fetuses cloned with fibroblast cells. #18, one B6D2F1 female cloned with a foetal fibroblast. #19, one (B6 × JF1)F1 male cloned with a foetal fibroblast. #20, one (B6 × JF1)F1 female cloned with a tail tip fibroblast. Two controls are fetuses obtained by IVF of C57BL/B6 and JF1 mice. (D) The methylation status of the *Not*I site in control placentas of B6D2F1 fetuses produced by ICSI and IVF. Five placentas each of ICSI fetuses and IVF fetuses were subjected to Southern blotting under the same conditions as in Fig. 1B. (E) The methylation degree of the *Not*I site evaluated by real time genomic PCR. The methylation levels evaluated by Southern blotting in Fig. 1B,D were confirmed by real time PCR using three of the placentas of cloned (closed circle) and control fetuses (open circle). For the controls (NM, IVF and ICSI), average methylation degrees of three placentas are shown. (F) Correlation between placental weight and methylation rate of 10 B6D2F1 fetuses cloned with cumulus cells. The placental weight and methylation rate of each cloned mouse are plotted. The methylation rate and placental weight show a positive correlation (coefficient r-value of 0.61, $P < 0.1$).